Chemical Communications

Electronic Supplementary Information (ESI)

Shape-persistent alleno-acetylenic macrocycle with modifiable periphery: Synthesis, chiroptical properties and H-bond-driven self-assembly into a homochiral columnar structure

Manolis D. Tzirakis, Nicolas Marion, W. Bernd Schweizer and François Diederich*

Laboratorium für Organische Chemie, ETH Zürich, Hönggerberg, Wolfgang-Pauli-Strasse 10, HCI, CH-8093 Zürich, Switzerland

* E-mail: diederich@org.chem.ethz.ch; Fax: +41 44 632 1109; Tel: +41 44 632 2992

Table of Contents **Page**

1. General Considerations

1.1. Materials

Reagents (ABCR, Acros, Aldrich, Fluka and TCI) were purchased as reagent grade and used without further purification. **Solvents** for flash column chromatography, plug filtrations and extraction were of technical grade and distilled before use. **Dry solvents** for reactions were purified by a solvent drying system (LC Technology Solutions Inc. SP-105) under nitrogen atmosphere (H_2O content < 10 ppm as determined by Karl-Fischer titration). All other solvents were purchased in *p.a.* quality. For all aqueous solutions, deionised water was used. **Reactions** on exclusion of air or water were performed in oven-dried glassware and under an Ar or N_2 atmosphere. **Flash column chromatography (FCC)** was carried out using silica gel (particle size: 40–63 μm, 230–400 mesh ASTM; Fluka). **Analytical thin layer chromatography (TLC)** was performed on aluminum sheets or glass plates coated with silica gel 60 F_{254} (Merck); visualisation with a UV lamp (254). **Evaporation *in vacuo*** was performed at 45–60 °C and 900–10 mbar. **Reported yields** refer to spectroscopically and chromatographically pure compounds that were dried under high vacuum (10^{-2} mbar) before analytical characterisation. **Nomenclature** follows the suggestions proposed by the computer program ACD Name by ACD Labs. The atoms were labelled arbitrarily, if necessary.

1.2. Physical Characterisation

^{1}H and ^{13}C nuclear magnetic resonance (NMR) spectra were recorded on Varian Gemini 300, Varian Mercury 300, Bruker ARX 300, Bruker DRX 400 and Bruker AV 400 spectrometers at 300 MHz or 400 MHz (^{1}H) and 75 MHz or 100 MHz (^{13}C), respectively. Chemical shifts (δ) are reported in ppm downfield from tetramethylsilane using the residual deuterated solvent signals as an internal reference ($CDCl_3$: δ_H = 7.26 ppm, δ_C = 77.16 ppm; $(CD_3)_2CO$: δ_H = 2.05 ppm, δ_C = 29.84 ppm; CD_3OD: $\delta_{H(Me)}$ = 3.31 ppm, δ_C = 49.00 ppm). For ^{1}H NMR, coupling constants J are given in Hz and the resonance multiplicity is described as s (singlet), d (doublet), t (triplet), q (quartet), quint (quintet), sext (sextet), sept (septet), m (multiplet) and br. (broad). All spectra were recorded at 25 °C. **UV/Vis spectra** were recorded on a Varian Cary-500 Scan spectrophotometer. The spectra were measured in a quartz cuvette (1 cm) at 25 °C. The absorption wavelengths are reported in nm with the extinction coefficient ε ($dm^3\ mol^{-1}\ cm^{-1}$) in brackets. **Circular Dichroism (CD) spectra** were recorded on a JASCO Corp. J-715, Rev. 1.00 instrument. **Optical rotations** were measured on a Perkin-Elmer 241 polarimeter. **Infrared (IR) spectra** were recorded on a

Perkin-Elmer 1600 FT-IR spectrometer (ATR, Golden Gate) and are reported as wavenumbers $\tilde{\nu}$ (cm^{-1}) with band intensities indicated as s (strong), m (medium), w (weak), very weak (vw), br. (broad) and sh (shoulder). **Mass spectrometry (MS) and high-resolution mass spectrometry (HR-MS)** was performed by the MS-service of the Laboratory for Organic Chemistry at the ETH Zürich on a Waters Micromass AutoSpec-Ultima spectrometer (EI), on a Bruker maXis spectrometer (ESI) or on a Varian IonSpec FT-ICR spectrometer (MALDI). For MALDI measurements, the matrix was 2-[(2*E*)-3-(4-*tert*-butylphenyl)-2-methylprop-2-enylidene]malononitrile (DCTB) or 3-hydroxypyridine-2-carboxylic acid (3-HPA). Masses are reported in *m*/*z* units as the molecule ion M^+, as $[M + H]^+$, $[M + Na]^+$ or $[M + K]^+$ with the corresponding intensities in %. **High-performance liquid chromatography (HPLC)** was run on a Merck-Hitachi LaChrom D-Line system equipped with a D-7000 Interface, an L-7100 pump and an L-7400 UV-detector.

2. Synthetic Procedure and Spectral Data of Compounds 2–11

2,6-Dimethyl-2,6-bis[4-(tetrahydro-2*H*-pyran-2-yloxy)phenyl]-4-heptyn-3-one (4).[1]

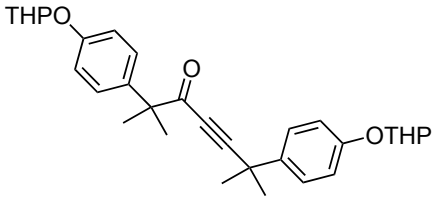

Compound **4** was obtained by following the previously reported protocol.[1]

$\tilde{\nu}_{max}$(neat)/cm^{-1} 2956 (sh), 2941 (br. m), 2873 (w), 2214 (m), 1669 (m), 1608 (m), 1582 (w), 1508 (s), 1454 (m), 1441 (m), 1384 (m), 1358 (m), 1291 (m), 1237 (s), 1201 (m), 1179 (s), 1146 (w), 1109 (s), 1075 (m), 1036 (m), 1021 (m), 964 (s), 919 (s), 887 (w), 872 (m), 830 (m), 816 (m), 770 (w), 729 (m), 647 (w); δ_H(300 MHz; $CDCl_3$; 298 K) 1.45 (s, 6H, C*Me*$_2$), 1.52–2.07 (m, 18H), 3.57–3.63 (m, 2H of THP), 3.86–3.94 (m, 2H of THP), 5.40 (dt, *J* = 9.9, 3.0 Hz, 2H, H–(C2) of THP), 6.89–6.93 (m, 2 arom. H), 7.03–7.08 (m, 4 arom. H), 7.21–7.26 ppm (m, 2 arom. H); δ_C(75 MHz; $CDCl_3$; 298 K) 19.02, 25.19, 25.43, 30.54, 30.90, 30.98, 35.76, 52.32, 62.05, 80.25, 96.12, 96.18, 96.24, 101.76, 115.99, 116.20, 126.15, 127.48, 135.98, 137.66, 155.37, 155.77, 190.86 ppm.

6-Methyl-6-(4-((tetrahydro-2*H*-pyran-2-yl)oxy)phenyl)-3-(2-(4-((tetrahydro-2*H*-pyran-2-yl)oxy)phenyl)propan-2-yl)-1-(triisopropylsilyl)hepta-1,4-diyn-3-yl 2,3,4,5,6-pentafluorobenzoate (5).

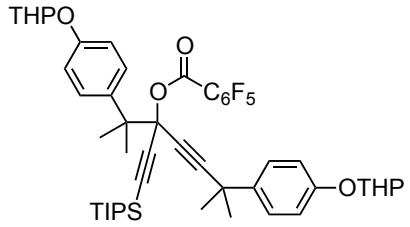

A solution of ethynyltriisopropylsilane (8.0 mL, 35.9 mmol) in THF (50 mL) was treated with *n*BuLi (1.6 M in hexane, 22.4 mL, 35.9 mmol) at –78 °C for 30 min. A solution of **4** (16.0 g, 32.6 mmol) in THF (30 mL) was added dropwise and the mixture stirred for 2 h at –78 °C. Pentafluorobenzoyl chloride (5.0 mL, 35.9 mmol) was added dropwise and the mixture stirred overnight, warming up to rt. The crude was washed twice with a saturated aqueous $NaHCO_3$ solution and extracted with MTBE. The combined organic layers were washed with brine, dried over $MgSO_4$ and evaporated. Flash column chromatography (SiO_2; pentane/EtOAc 95:5) gave **5** (20.5 g, 70%) as an extremely viscous yellow oil.

$\tilde{\nu}_{max}$(neat)/cm^{-1} 2943 (m), 2866 (w), 1753 (m), 1652 (w), 1609 (w), 1507 (s), 1464 (m), 1386 (w), 1358 (w), 1326 (m), 1290 (w), 1240 (s), 1204 (s), 1180 (s), 1146 (w), 1125 (m), 1110 (m), 1075 (m), 1038 (m), 1020 (m), 1000 (s), 964 (s), 921 (s), 876 (m), 873 (m), 830 (m), 788 (w), 764 (w), 731 (w), 712 (w), 677 (m); δ_H(300 MHz; $CDCl_3$; 298 K; mixture of stereoisomers) 1.13 (br s, 21H; $Si(CHMe_2)_3$), 1.56 (s, 3H, C*H*$_3$), 1.58 (s, 3H, C*H*$_3$), 1.62–1.73 (m, 6H of THP), 1.73 (s, 6H, 2 × C*H*$_3$), 1.86–1.91 (m, 4H of THP), 1.98–2.13 (m, 2H of THP), 3.59–3.67 (m, 2H of THP), 3.90–4.00 (m, 2H of THP), 5.41–5.43 (m, 2H, H–(C2) of THP), 6.94 (d, J = 8.7 Hz, 2 arom. H), 7.01 (d, J = 8.7 Hz, 2 arom. H), 7.43 (d, J = 8.7 Hz, 2 arom. H), 7.52 ppm (d, J = 8.7 Hz, 2 arom. H); δ_C(75 MHz; $CDCl_3$; 298 K; mixture of stereoisomers) 11.48, 18.75, 19.05, 19.10, 24.36, 24.58, 24.60, 25.48, 30.61, 31.38, 31.44, 31.51, 35.76, 46.02, 61.98, 62.07, 76.64, 77.07, 77.49, 77.60, 89.51, 89.52, 94.58, 96.21, 96.22, 96.36, 101.80, 114.71, 115.91, 126.42, 129.77, 135.28, 139.16, 155.25, 155.57 ppm; δ_F(282 MHz; $CDCl_3$; 298 K) –159.67 (m), –148.77 (m), –137.82 ppm (m); HR-MALDI-MS (3-HPA): *m*/*z* (%): 905.3630 (20, $[M + K]^+$, calcd for $C_{49}H_{59}F_5O_6KSi^+$: 905.3633), 889.3891 (28, $[M + Na]^+$, calcd for $C_{49}H_{59}F_5O_6NaSi^+$: 889.3893), 391 (100).

(*M*/*P*)-2-Methyl-5,7-bis(2-{4-[((2*R*/*S*)-tetrahydro-2*H*-pyran-2-yl)oxy]phenyl}isopropyl)-9-(triisopropylsilyl)nona-5,6-dien-3,8-diyn-2-ol (6).

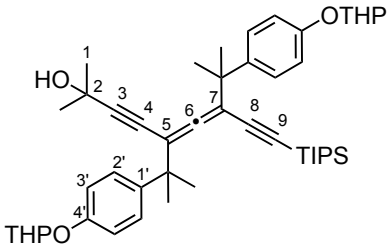

A solution of **5** (2.45 g, 2.8 mmol) in toluene (24 mL) was treated with *i*Pr_2NEt (1.1 mL, 5.9 mmol), degassed with N_2 for 20 min, treated sequentially with 2-methyl-3-butyn-2-ol (0.55 mL, 5.6 mmol), [$Pd(PPh_3)_4$] (173 mg, 0.15 mmol) and CuI (57 mg, 0.3 mmol) and heated to 80 °C for 2 days. After evaporation of toluene under reduced pressure, the mixture was diluted with pentane, washed twice with H_2O, dried over $MgSO_4$ and evaporated. Flash column chromatography (SiO_2; pentane/EtOAc 85:15) gave **6** (1.24 g, 60%) as a highly viscous orange oil.

R_f = 0.21 (SiO_2; hexane/EtOAc 85:15); δ_H(300 MHz; $CDCl_3$; 298 K; mixture of diastereoisomers) 1.02 and 1.03 (2 br. s, 21 H; Si(CHMe_2)$_3$), 1.41–1.48 (several s, 18 H; 3 CMe_2), 1.57–1.72 (m, 6 H of THP), 1.83–1.89 (m, 4 H of THP), 1.96–2.04 (m, 2 H of THP), 2.19–2.28 (2 br. s, 1 H; OH), 3.54–3.62 (m, 2 H of THP), 3.85–3.95 (m, 2 H of THP), 5.36–5.42 (m, 2 H; 2 × H-C(2) of THP), 6.92–6.96 (m, 4 arom. H), 7.13–7.21 ppm (m, 4 arom. H); δ_C(101 MHz; $CDCl_3$; 298 K; mixture of diastereoisomers) 11.62 (3 C; Si(*C*HMe_2)$_3$), 18.94 (6 C; Si(CH*Me*$_2$)$_3$), 19.04, 19.13 and 19.22 (2 C; 2 C(4) of THP)), 25.58 (2 C; 2 C(5) of THP), 28.48, 28.54, 28.64, 28.71, 28.89 and 28.96 (2 C; 2 C(3) of THP), 30.67, 30.73, 31.62 (C*Me*$_2$OH), 42.90, 42.96, 43.11 and 43.16 (2 C; 2 *C*Me_2), 61.94, 62.01 and 62.17 (2 C; 2 C(6) of THP), 65.58 and 65.65 (C(2)), 76.15 and 76.23 (C(4)), 94.72 and 94.79 (C≡*C*Si), 96.08, 96.28, 96.42 and 96.56 (2 C; 2 C(2) of THP), 97.60, 97.65 and 97.68 (C(3)), 100.29 (C(8)), 103.15, 103.22, 104.51, 104.54 and 104.58 (2 C; C(5,7)), 115.63, 115.75 and 115.80 (4 C; 2 C(3',5')), 127.42 and 127.47 (4 C; 2 C(2',6')), 139.81, 139.83, 139.86 and 139.97 (2 C; 2 C(1')), 155.00 and 155.12 (2 C; 2 C(4')), 212.56, 212.70 ppm (C(6)); $\tilde{\nu}_{max}$(neat)/cm^{-1} 2943 (m), 2865 (m), 2251 (m), 2141 (w), 1732 (m), 1608 (m), 1509 (s), 1463 (m), 1360 (m), 1236 (s), 1202 (m), 1180 (m), 1125 (m), 1109 (m), 1073 (m), 1037 (m), 1021 (m), 968 (m), 907 (s), 882 (m), 830 (m), 728 (s), 676 (m), 647 (m), 606 (w); HR-MALDI-MS (3-HPA): *m*/*z* (%): 762.4595 (35),

761.4570 (64, [*M* + Na]$^+$, calcd for $C_{47}H_{66}NaO_5Si^+$: 761.4572), 705.8373 (21), 679.2081 (22), 595.0141 (20), 504.1234 (23), 503.1187 (85), 263.0540 (99), 241.0720 (100).

(*M*/*P*)-(±)-2-Methyl-5,7-bis[2-(4-hydroxyphenyl)isopropyl]-9-(triisopropylsilyl)nona-5,6-dien-3,8-diyn-2-ol ((±)-7).

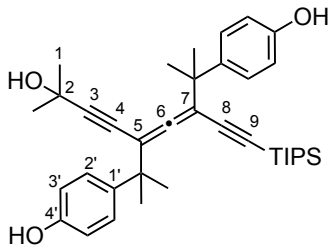

To a THF (70 mL) solution of **6** (1 g, 1.35 mmol) at 0 ºC, H_2O (30 mL) and $HCl_{conc.}$ (6 mL) were added and the solution was stirred for 2 h. The mixture was poured in an aqueous saturated NH_4Cl/MTBE 1:1 solution, extracted with MTBE, dried over $MgSO_4$ and concentrated *in vacuo*. The crude product was purified by flash column chromatography (SiO_2; hexane/EtOAc 7:3) to afford (±)-**7** as an off-white solid (554 mg, 72%). The partially deprotected product was also isolated and was treated under the same conditions to increase the yield of (±)-**7**.

R_f = 0.43 (SiO_2; hexane/EtOAc 3:2); $\tilde{\nu}_{max}$(neat)/cm^{-1} 3330 (br), 2941 (s), 2864 (s), 2141 (m), 1613 (m), 1596 (m), 1512 (s), 1461 (s), 1381 (m), 1362 (m), 1298 (w), 1232 (s), 1179 (s), 1105 (w), 1069 (m), 1015 (m), 995 (m), 955 (m), 909 (m), 881 (s), 829 (s), 765 (m), 731 (m), 707 (m), 675 (m), 662 (m); δ_H(300 MHz; $CDCl_3$; 298 K) 1.03 (br. s, 21 H; Si(CHMe$_2$)$_3$), 1.36 (s, 3 H; Me), 1.436, 1.448, 1.451 and 1.463 (4 s, 12 H; 4 Me), 1.51 (s, 3 H; Me), 2.18 (br. s, 1 H; propargylic OH), 5.1–5.4 (br. s, 2 H; 2 phenolic OH), 6.70 (d, *J* = 8.8 Hz, 2 H; H-C(3',5')), 6.74 (d, *J* = 8.8 Hz, 2 H; H-C(3',5')), 6.97 (d, *J* = 8.8 Hz, 2 H; H-C(2',6')), 7.12 ppm (d, *J* = 8.8 Hz, 2 H; H-C(2',6')); δ_C(75 MHz; $CDCl_3$; 298 K) 11.68 (3 C; Si(*C*HMe$_2$)$_3$), 18.97 (6 C; Si(CH*Me*$_2$)$_3$), 28.02, 28.21, 29.18 and 29.54 (4 C; 2 C*Me*$_2$), 31.36 and 31.59 (2 C; C*Me*$_2$OH), 43.06 and 43.11 (2 C; 2*C*Me$_2$Ar), 66.11 (C(2)), 76.51 (C(4)), 94.93 (C(9)), 97.36 (C(3)), 100.21 (C(8)), 102.99 and 104.84 (2 C; C(5,7)), 114.68 and 114.69 (4 C; 2 C(3',5')), 127.69 and 127.91 (4 C; 2 C(2',6')), 138.75 and 138.92 (2 C; 2 C(1')), 153.60 and 153.69 (2 C; 2 C(4')), 212.82 ppm (C(6)). HR-ESI-MS: *m*/*z* (%): 609.3156 (73, [*M* + K]$^+$, calcd for $C_{37}H_{50}KO_3Si^+$: 609.3161), 593.3417 (100, [*M* + Na]$^+$, calcd for $C_{37}H_{50}NaO_3Si^+$: 593.3421).

(*M*/*P*)-(±)-2-Methyl-5,7-bis[2-(4-hydroxyphenyl)isopropopyl]nona-5,6-dien-3,8-diyn-2-ol ((±)-2).

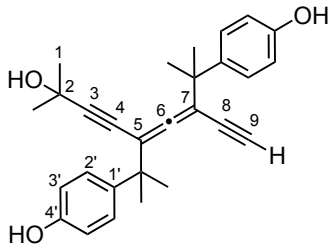

A solution of (±)-**7** (100 mg, 0.17 mmol) in THF (10 mL) was treated with 1 M nBu$_4$NF in THF (0.17 mL) at 0 ºC, stirred for 2 h, diluted with water and extracted with MTBE. The organic layer was dried over $MgSO_4$ and evaporated. Flash column chromatography (SiO_2; hexane/EtOAc 7:3 → 5:5) yielded (±)-**2** (63 mg, 90%) as an off-white solid.

R_f = 0.15 (SiO_2; hexane/EtOAc 3:2); m.p. 170–174 °C (decomp); λ_{max}(CH_3CN)/nm 282 (ε/dm^3 mol^{-1} cm^{-1} 3613), 276 (4705), 224 (37718); $\tilde{\nu}_{max}$(neat)/cm^{-1} 3548 (br), 3345 (br), 3269 (s), 3254 (s), 3118 (br), 2978 (s), 2962 (s), 2928 (m), 2871 (m), 2798 (w), 2686 (w), 2610 (w), 1935 (vw), 1609 (m), 1600 (m), 1512 (s), 1455 (m), 1380 (m), 1362 (m), 1296 (w), 1256 (s), 1241 (s), 1190 (m), 1178 (s), 1156 (s), 1105 (m), 1089 (m), 1041 (m), 1013 (m), 957 (m), 938 (m), 927 (m), 918 (m), 878 (m), 835 (s), 820 (s), 803 (m), 747 (m), 730 (m), 717 (m), 681 (m), 661 (s), 650 (s), 624 (m); δ_H(300 MHz; $(CD_3)_2CO$; 298 K) 1.39, 1.40, 1.41, 1.42, 1.43 and 1.45 (6 s, 18 H; 3 CMe_2), 3.43 (s, 1 H; C≡CH), 4.36 (br. s, 1 H; propargylic OH), 6.75 (d, J = 8.8 Hz, 4 H; 2 H–C(2',6')), 7.1 (d, J = 8.8 Hz, 2 H; 2 H–C(3',5')), 7.14 (d, J = 8.8 Hz, 2 H; 2 H–C(3',5')), 8.17 ppm (br. s, 2 H; 2 phenol OH); δ_C(75 MHz; $(CD_3)_2CO$; 298 K) 28.85, 28.93 and 29.05 (4 C; 2 CMe_2Ar), 31.95 and 31.98 (2 C; CMe_2OH), 43.00 and 43.16 (2 C; 2 CMe$_2$), 65.12 (C(2)), 75.25 (C(4)), 78.30 (C(8)), 82.56 (C(9)), 100.37 (C(3)), 103.68 and 105.18 (2 C; C(5,7)), 115.44 and 115.54 (4 C; 2 C(3',5')), 128.27 and 128.32 (4 C; 2 C(2',6')), 138.34 and 138.38 (2 C; 2 C(1')), 156.48 and 156.53 (2 C; 2 C(4')), 213.93 ppm (C(6)); HR-ESI-MS: m/z (%): 453.1827 (61, $[M + K]^+$, calcd for $C_{28}H_{30}KO_3^+$: 453.1827), 438.2125 (30), 437.2084 (73, $[M + Na]^+$, calcd for $C_{28}H_{30}NaO_3^+$: 437.2087), 398.2197 (31), 397.2161 (100, $[M – OH]^+$, calcd for $C_{28}H_{29}O_2^+$: 397.2162), 268.9985 (50).

(*P*,*P*)-(+)-5,7,12,14-Tetrakis{2-[4-(methoxymethoxy)phenyl]isopropyl}-2,17-dimethyloctadeca-5,6,12,13-tetraen-3,8,10,15-tetrayne-2,17-diol ((*P*,*P*)-(+)-9).

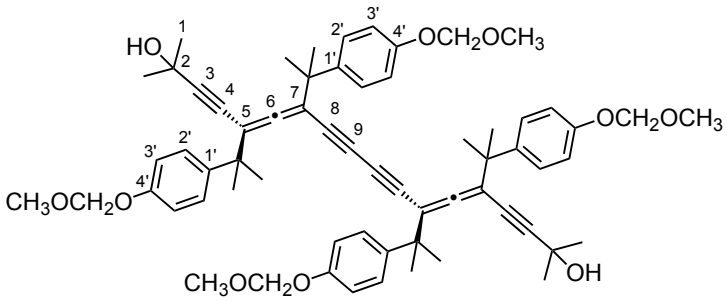

A mixture of enantiopure (*P*)-(+)-**2** (200 mg, 0.48 mmol) in methyl *tert*-butyl ether (MTBE; 6 mL) and NaOH (400 mg, 21 equiv.) in water (3 mL) was stirred at rt for 20 min in the presence of Adogen® 464 [methyltrioctylammonium chloride; 100 μL] as phase-transfer catalyst. Chloromethyl methyl ether (1.76 mL, 20 equiv.) was gradually added until the reaction was complete. The mixture was diluted with water and extracted with MTBE. The combined organic extracts were dried (Na_2SO_4) and evaporated. *It is important to note that the resulting product* (*P*)-(+)-**8** *is highly unstable when stored neat at rt for few minutes*. Thus, the resulting amber oil was immediately dissolved in acetone and engaged in the next step without further purification.

Copper(I) chloride–N,N,N′,N′-tetramethylethylenediamine complex: A deaerated solution of copper(I) chloride (1.2 g, 12 mmol) in acetone (30 mL) atmosphere was treated under nitrogen with *N,N,N′,N′*-tetramethylethylenediamine (TMEDA) (1.5 mL, 10 mmol) for 30 min. The solution was filtered to give a clear deep-blue-green solution of the CuCl/TMEDA catalyst that was immediately used in the oxidative coupling reaction.

A solution of (*P*)-(+)-**8** in acetone (20 mL) under air atmosphere was treated with the solution of CuCl/TMEDA catalyst in acetone (30 mL) for 2 h. The mixture was poured into a saturated aqueous NH_4Cl solution (50 mL) and extracted with Et_2O (4 × 50 mL). The combined organic layers were dried over Na_2SO_4, filtered and evaporated. Flash column chromatography (SiO_2; hexane/AcOEt 4:6) gave (*P*)-(+)-**9** (168 mg, 70%) as a highly viscous amber oil.

$[a]_D^{20}$ +250 (*c* 0.1, CH_3CN); R_f = 0.16 (SiO_2; hexane/EtOAc 2:3); $\lambda_{max}(CH_3CN)$/nm 319 (ε/dm^3 mol^{-1} cm^{-1} 15910), 299 (18940), 280 (22480), 261 (54840), 252 (58450), 224 (61950); $\tilde{\nu}_{max}$(neat)/cm^{-1} 3444 (br), 2970 (s), 2930 (m), 2902 (m), 2826 (w), 1920 (vw), 1717 (br), 2128 (vw), 1608 (m), 1582 (w), 1509 (s), 1463 (m), 1443 (m), 1406 (m), 1383 (m), 1362 (m), 1307 (m), 1288 (w), 1233 (s), 1202 (m), 1179 (s), 1150 (s), 1112 (m), 1076 (s), 998 (s), 957 (m), 920 (m), 881 (w),

831 (s), 731 (s), 651 (m); δ_H(300 MHz; CD_3OD; 298 K) 1.29–1.46 (several s, 18 H; 3CMe_2), 3.439 and 3.445 (2 s, 6 H; 2 OMe), 5.16 and 5.17 (2 s, 4 H; 2 OCH_2O), 6.93 (br. d, 2 arom. H; J = 9.0 Hz), 6.96 (br. d, 2 arom. H; J = 8.7 Hz), 7.14 (br. d, 2 arom. H; J = 9.0 Hz), 7.15 ppm (br. d, 2 arom. H; J = 8.7 Hz); δ_C(75 MHz; $CDCl_3$; 298 K) 28.48, 28.79, 28.86 and 29.10 (4 C; 2 CMe_2Ar), 31.52 and 31.56 (2 C; CMe_2OH), 43.12 and 43.24 (2 C; 2 CMe$_2$Ar), 56.08 and 56.14 (2 C; 2 OMe), 65.55 (C(2)), 75.45 and 75.51 (2 C; C(4,9)), 77.69 (C(8)), 94.39 and 94.42 (2 C; 2 OCH_2O), 98.75 (C(3)), 103.59 and 104.34 (2 C; C(5,7)), 115.51 and 115.61 (4 C; 2 C(3',5')), 127.45 and 127.47 (4 C; 2 C(2',6')), 139.77 and 139.87 (2 C; 2 C(1')), 155.24 and 155.35 (2 C; 2 C(4')), 214.54 ppm (C(6)); HR-ESI-MS: m/z (%): 1020.5609 (100, $[M + NH_4]^+$, calcd for $C_{64}H_{78}NO_{10}^+$: 1020.5620).

The enantiomer (*M*,*M*)-(–)-**9** was prepared in a similar way, starting from (*M*)-(–)-**2**: $[a]_D^{20}$ –250 (*c* 0.1, CH_3CN).

(*P*,*P*)-(+)-3,5,10,12-Tetrakis{2-[4-(methoxymethoxy)phenyl]isopropyl}tetradeca-3,4,10,11-tetraen-1,6,8,13-tetrayne ((*P*,*P*)-(+)-10).

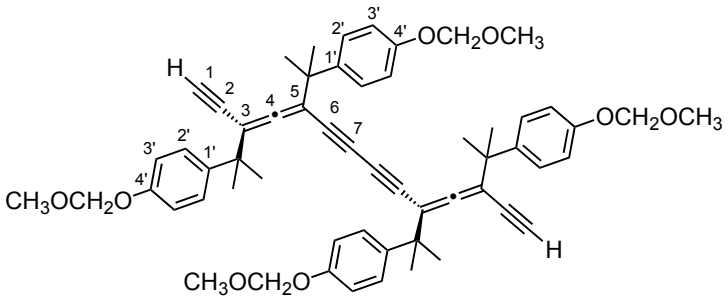

Pulverised NaOH (180 mg, 4.5 mmol) was placed in a Schlenk tube and dried with a heat gun under vacuum (0.1 Torr). The tube was filled with N_2 and a solution of (*P*,*P*)-(+)-**9** (30 mg, 0.03 mmol) in dry toluene (2 mL) was transferred to the Schlenk tube. The mixture was heated to 90 ºC until TLC showed almost complete disappearance of (*P*,*P*)-(+)-**9**. The mixture was cooled to 20 °C, diluted with hexane and washed with a saturated aqueous NH_4Cl solution (10 mL). The organic phase was dried over Na_2SO_4, filtered and evaporated. Flash column chromatography (SiO_2; hexane/EtOAc 7:3) gave (*P*,*P*)-(+)-**10** (19 mg, 70%) as a highly viscous amber oil.

$[a]_D^{20}$ +181 (*c* 0.1, $CHCl_3$); R_f = 0.51 (SiO_2; hexane/EtOAc 3:2); λ_{max}(CH_3CN)/nm 320 (ε/dm^3 mol^{-1} cm^{-1} 17850), 300 (20640), 281 (24160), 262 (58970), 251 (70570), 240 (60940); $\tilde{\nu}_{max}$(neat)/cm^{-1} 3283 (br), 2968 (m), 2930 (m), 2898 (m), 2825 (w), 2097 (vw), 1921 (vw), 1608 (m), 1582 (w), 1509 (s), 1463 (m), 1443 (m), 1406 (w), 1384 (m), 1363 (m), 1307 (m), 1288 (m), 1233

(s), 1202 (m), 1180 (m), 1150 (s), 1112 (m), 1076 (s), 997 (s), 920 (s), 831 (s), 787 (w), 759 (m), 732 (m), 649 (m), 635 (m), 613 (m); δ_H(400 MHz; $CDCl_3$; 298 K) 1.40 (s, 3 H; Me), 1.456, 1.463 and 1.47 (3 s, 9 H; 3 Me), 2.93 (1 s, 1 H; C≡CH), 3.47 and 3.48 (2 s, 6 H; 2 OMe), 5.16 and 5.17 (2 s, 4 H; 2 OCH_2O), 6.95 (br. d, 2 arom. H; J = 6.6 Hz), 6.97 (br. d, 2 arom. H; J = 6.6 Hz), 7.14 (br. d, 2 arom. H; J = 6.6 Hz), 7.21 ppm (br. d, 2 arom. H; J = 6.6 Hz); δ_C(101 MHz; $CDCl_3$; 298 K) 28.41, 28.71, 28.75 and 28.88 (4 C; 2 CMe_2), 42.86 and 43.18 (2 C; 2 CMe$_2$), 56.12 (2 C; 2 OMe), 75.35, 76.99, 78.01, 81.84 (C(1)), 94.63 (2 C; 2 OCH_2O), 103.96 and 104.18 (2 C; C(3,5)), 115.85 and 115.90 (4 C; 2 C(3',5')), 127.64 and 127.67 (4 C; 2 C(2',6')), 139.91 and 139.94 (2 C; 2 C(1')), 155.79 and 155.85 (2 C, 2 C(4')), 216.07 ppm (C(4)); HR-MALDI-MS (3-HPA): m/z (%): 925.4078 (100, $[M + K]^+$, calcd for $C_{58}H_{62}KO_8^+$: 925.4076), 909.4336 (36, $[M + Na]^+$, calcd for $C_{58}H_{62}NaO_8^+$: 909.4337), 886.4439 (30, M^+, calcd for $C_{58}H_{62}O_8^+$: 886.4439).

The enantiomer (*M*,*M*)-(–)-**10** was prepared in a similar way, starting from (*M*,*M*)-(–)-**9**: $[a]_D^{20}$ –173 (*c* 0.1, $CHCl_3$).

(*P*,*P*,*P*,*P*)-(–)-1,3,8,10,15,17,22,24-Octakis{2-[4-(methoxymethoxy)phenyl]isopropyl} cyclooctacosa-1,2,8,9,15,16,22,23-octaen-4,6,11,13,18,20,25,27-octayne ((*P*,*P*,*P*,*P*)-(–)-(11).

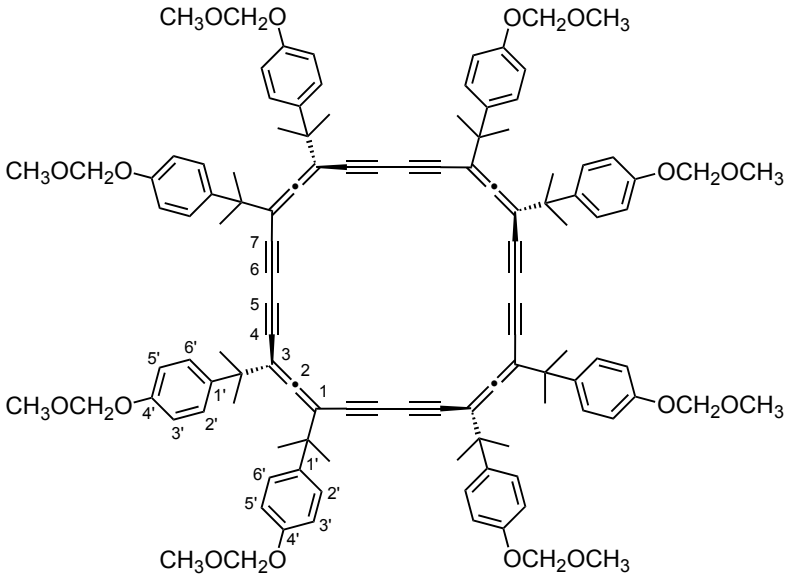

A solution of CuCl (1.12 g, 11.3 mmol) and $CuCl_2$ (151 mg, 1.12 mmol) in pyridine (170 mL) was degassed by bubbling Ar for 60 min. A solution of (*P*,*P*)-(+)-**10** (50 mg, 0.056 mmol) in pyridine (50 mL) was added over a period of 20 h. After the addition, the mixture was stirred at rt for 3 h. After evaporation of pyridine, the solution of the solid residue in saturated aqueous NH_4Cl solution

(40 mL) and extracted with pentane. The organic layer was dried over Na_2SO_4 and evaporated. Flash column chromatography (SiO_2; hexane → hexane/EtOAc 3:2) gave (*P*,*P*,*P*,*P*)-(–)-**11** (32 mg, 65%) as an off-white solid.

$[a]_D^{20}$ –245 (*c* 0.1, CH_3CN); R_f = 0.47 (SiO_2; hexane/EtOAc 6:4); $\lambda_{max}(CH_3CN)$/nm 326 (ε/dm^3 mol^{-1} cm^{-1} 21670), 304 (38290), 284 (sh, 66660), 247 (141820), 224 (139020); $\tilde{\nu}_{max}$(neat)/cm^{-1} 2967 (w), 2926 (w), 2825 (w), 2100 (vw), 1920 (vw), 1706 (w), 1608 (w), 1582 (w), 1509 (s), 1463 (w), 1406 (w), 1384 (w), 1363 (w), 1307 (w), 1288 (w), 1234 (s), 1202 (m), 1180 (m), 1150 (s), 1101 (w), 1076 (s), 994 (s), 921 (m), 831 (s), 752 (s), 666 (w), 654 (w), 614 (w); δ_H(300 MHz; $CDCl_3$; 298 K) 1.41 (s, 6 H, 2 Me), 1.49 (s, 6 H; 2 Me), 3.48 (s, 6 H; 2 OMe), 5.18 (s, 4 H; 2 OCH_2O), 6.95 (d, *J* = 8.7 Hz; 4 H; 2 H–C(3',5')), 7.15 ppm (d, *J* = 8.7 Hz; 4 H; 2 H–C(2',6')); δ_C(75 MHz; $CDCl_3$; 298 K) 28.65 and 29.42 (4 C; 2 C*Me*$_2$), 43.18 (2 C; 2 *C*Me$_2$), 56.21 (2 C; 2 OMe), 75.35 (2 C, C(5,6)), 78.47 (2 C; C(4,7)), 94.47 (2 C; 2 OCH_2O), 104.41 (2 C; C(1,3)), 115.68 (4 C; 2 C(3',5')), 127.43 (4 C; 2 C(2',6')), 139.58 (2 C; 2 C(1')), 155.45 (2 C; 2 C(4')), 218.04 ppm (C; C(2)); HR-MALDI (DCTB): *m*/*z* (%): 1769.8578 (100, $[M + H]^+$, calcd for $C_{116}H_{121}O_{16}^+$: 1769.8649), 1768.8533 (80, M^+, calcd for $C_{116}H_{120}O_{16}^+$: 1768.8571).

The enantiomer (*M*,*M*,*M*,*M*)-(+)-**11** was prepared in a similar way, starting from (*M*,*M*)-(–)-**10**: $[a]_D^{20}$ +255 (*c* 0.1, CH_3CN).

(*P*,*P*,*P*,*P*)-(–)-1,3,8,10,15,17,22,24-Octakis[2-(4-hydroxyphenyl)isopropyl] cyclooctacosa-1,2,8,9,15,16,22,23-octaen-4,6,11,13,18,20,25,27-octayne ((*P*,*P*,*P*,*P*)-(–)-(3).

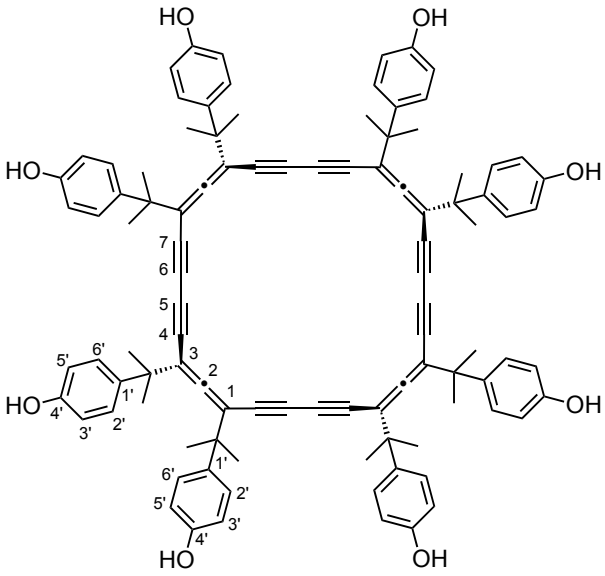

A solution of (*P*,*P*,*P*,*P*)-(–)-**11** (32 mg, 18 μmol) in THF (3 mL) was treated with 6 M HCl (0.01 mL) for 12 h at rt. The mixture was poured into distilled water (10 mL) and extracted with Et_2O (4 × 10 mL). The combined organic layers were dried over Na_2SO_4 and evaporated. Flash column chromatography (SiO_2; CH_2Cl_2 → CH_2Cl_2/MeOH 95:5) gave (*P*,*P*,*P*,*P*)-(–)-**3** (23 mg, 90%) as a white solid.

$[a]_D^{20}$ –243 (*c* 0.1, CH_3CN); R_f = 0.10 (SiO_2; CH_2Cl_2/MeOH 95:5); m.p. > 200 °C (decomp); $\lambda_{max}(CH_3CN)$/nm 326 (ε/dm^3 mol^{-1} cm^{-1} 14175), 303 (30590), 286 (sh, 53570), 276 (sh, 64190), 247 (116550), 227 (120770); $\tilde{\nu}_{max}$(neat)/cm^{-1} 2969 (w), 2930 (w), 2870 (w), 1699 (w), 1612 (m), 1596 (w), 1511 (s), 1459 (w), 1437 (w), 1384 (w), 1363 (w), 1297 (w), 1229 (br. s), 1178 (s), 1100 (w), 1062 (w), 1013 (w), 908 (w), 829 (s), 730 (m), 668 (w), 633 (w); δ_H(300 MHz; $(CD_3)_2CO$; 298 K) 1.40 (s, 6 H, 2 Me), 1.47 (s, 6 H; 2 Me), 6.77 (br. d, *J* = 8.7 Hz; 4 H; 2 H–C(3',5')), 7.08 (br. d, *J* = 8.7 Hz; 4 H; 2 H–C(2',6')), 8.26 ppm (s, 2 H; 2 OH); δ_C(75 MHz; $(CD_3)_2CO$; 298 K) 29.59 and 30.18 (4 C; 2 C*Me*$_2$), 44.36 (2 C; 2 *C*Me$_2$), 77.15 (2C, C(5,6)), 79.21 (2 C; C(4,7)), 106.35 (2 C; C(1,3)), 116.63 (4 C; 2 C(3',5')), 129.03 (4 C; 2 C(2',6')), 138.52 (2 C; 2 C(1')), 157.51 (2 C; 2 C(4')), 219.71 ppm (C; C(2)); HR-MALDI (DCTB): *m*/*z* (%): 1439.6365 (100, $[M + Na]^+$, calcd for $C_{100}H_{88}NaO_8^+$: 1439.6371), 1416.6466 (27, M^+, calcd for $C_{100}H_{88}O_8^+$: 1416.6474).

The enantiomer (*M*,*M*,*M*,*M*)-(+)-**3** was prepared in a similar way, starting from (*M*,*M*,*M*,*M*)-(+)-**11**: $[a]_D^{20}$ +250 (*c* 0.1, CH_3CN).

3. Optical Resolution of (±)-2 and CD Spectra of (*P*)-(+)-2 and (*M*)-(–)-2

Enantiomers (*P*)-(+)-**2** and (*M*)-(–)-**2** were resolved from the racemate by preparative HPLC using a chiral stationary phase (Chiralpak® IA from Diacel Chemical Industries Ltd.); the presence of unprotected phenol moieties in addition to the $C(CH_3)_2OH$-protected acetylene group were essential for the chiral separation of (±)-**2**. The mobile phase was eluted isocratically with *n*-hexane/*i*PrOH 87.5:12.5 at a flow of 18 mL min^{-1}. Under these conditions, a sample of (±)-**2** (20 mg dissolved in 2 mL of *n*-hexane/*i*PrOH 87.5:12.5) was resolved into the two enantiomers:

(*P*)-(+)-**2**: t_R = 47 min, e.r. > 99:1, $[a]_D^{20}$ +90 (*c* 0.1, CH_3CN).

(*M*)-(–)-**2**: t_R = 61 min, e.r. > 99:1, $[a]_D^{20}$ –85 (*c* 0.1, CH_3CN).

The absolute configuration was unambiguously assigned by ECD spectroscopy, as similar (*P*)-configured 1,3-DEAs exhibit a positive Cotton effect around 225 nm.[2]

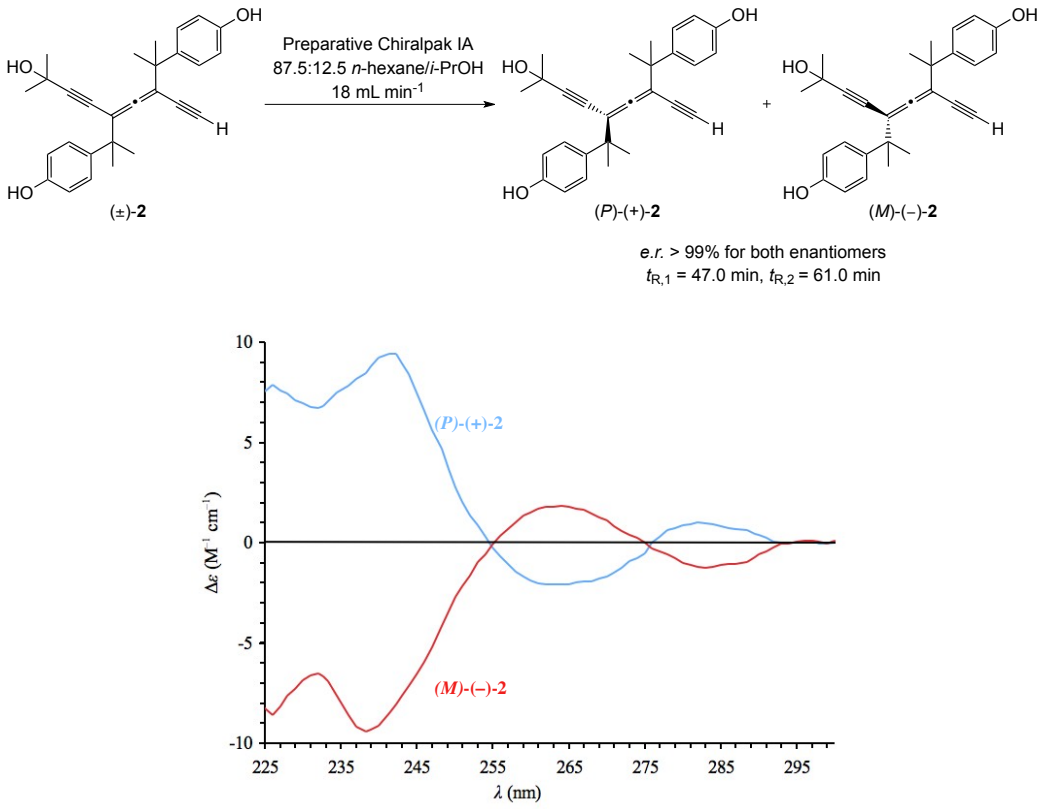

Figure S1. Optical resolution (top) and CD spectrum (bottom) of (*P*)-(+)-**2** (e.r. > 99:1, blue line) and (*M*)-(–)-**2** (e.r. > 99:1, red line). CD spectra were recorded in $CHCl_3$ at 25 ºC with C = 2.5 × 10^{-5} M.

4. Concentration-Dependent ^{1}H NMR Measurements

Concentration-dependent ^{1}H NMR measurements were performed for (±)-**7** (Fig. S2), (±)-**2** (Fig. S3 and S4) and (*P*,*P*,*P*,*P*)-(–)-**3** (Fig. S5 and S6) in $CDCl_3$, 1,1,2,2-tetrachloroethane-d_2 or chlorobenzene-d_5 at 25 ºC. These measurements showed a downfield shift of phenolic OH protons with increasing concentrations accompanied by sharp changes in the splitting pattern of the aromatic protons and significant line broadening. The downfield shift of the OH protons is a typical feature of protons involved in hydrogen bonds. Further evidence of the existence of H-bonding interactions was obtained by performing the same measurements in acetone-d_6, a well-known, hydrogen-bond-breaking polar solvent; in this case no concentration-dependent changes were observed in the chemical shifts of either the OH or aromatic protons of (±)-**7**, (±)-**2** and (*P*,*P*,*P*,*P*)-(–)-**3**. In addition to H-bonding interactions, π-π and dipole-dipole interactions between adjacent molecules could also contribute, albeit to a much lesser extend if not at all.

It should be noted that (±)-**2** is a highly polar compound (R_f = 0.15; SiO_2, hexane/EtOAc 3:2) with negligible solubility in solvents such as pentane, hexanes, toluene, dichloromethane and chloroform. The presence of a small amount of a polar co-solvent, such as acetone or EtOAc, increased the solubility of (±)-**2** in the aforementioned apolar solvents and allowed, for example, ^{1}H NMR studies to be performed in $CDCl_3$ (Fig. S3). However, these latter studies could be performed only when the samples were measured shortly after their preparation, since a few minutes later a complete aggregation occurred. Also, the use of 1,1,2,2-tetrachloroethane-d_2 allowed for performing the corresponding ^{1}H NMR measurements in the absence of a polar co-solvent (Fig. S4). In this case, the solubility of (±)-**2** was greatly enhanced by heating the corresponding sample at 70–80 ºC for 1–2 min, though similar to the case of $CDCl_3$, aggregation of (±)-**2** was still observed upon storage at rt for few minutes. The employment of another non-polar aprotic solvent, such as chlorobenzene-d_5, gave similar results to 1,1,2,2-tetrachloroethane-d_2, although in this case the aromatic protons of (±)-**2** were partially overlapped by the residual solvent peaks (spectra not shown).

Similarly, macrocycle (*P*,*P*,*P*,*P*)-(–)-**3** is a highly polar compound (R_f = 0.1; SiO_2, CH_2Cl_2/MeOH 95:5) and, as a result, concentration-dependent ^{1}H NMR measurements could be performed in $CDCl_3$ only when the samples were measured shortly after their preparation in the presence of a small amount of a polar co-solvent, such as acetone (Fig. S5). Also, similar to the case of (±)-**2**, the use of 1,1,2,2-tetrachloroethane-d_2 allowed for performing the corresponding ^{1}H NMR measurements in the absence of a polar co-solvent (Fig. S6). In this case, the solubility of (±)-**3** was enhanced by heating the corresponding solution at 90–100 ºC for 1–2 min. However, a

significant aggregation of (±)-**3** was still observed upon storage at rt for a few minutes.

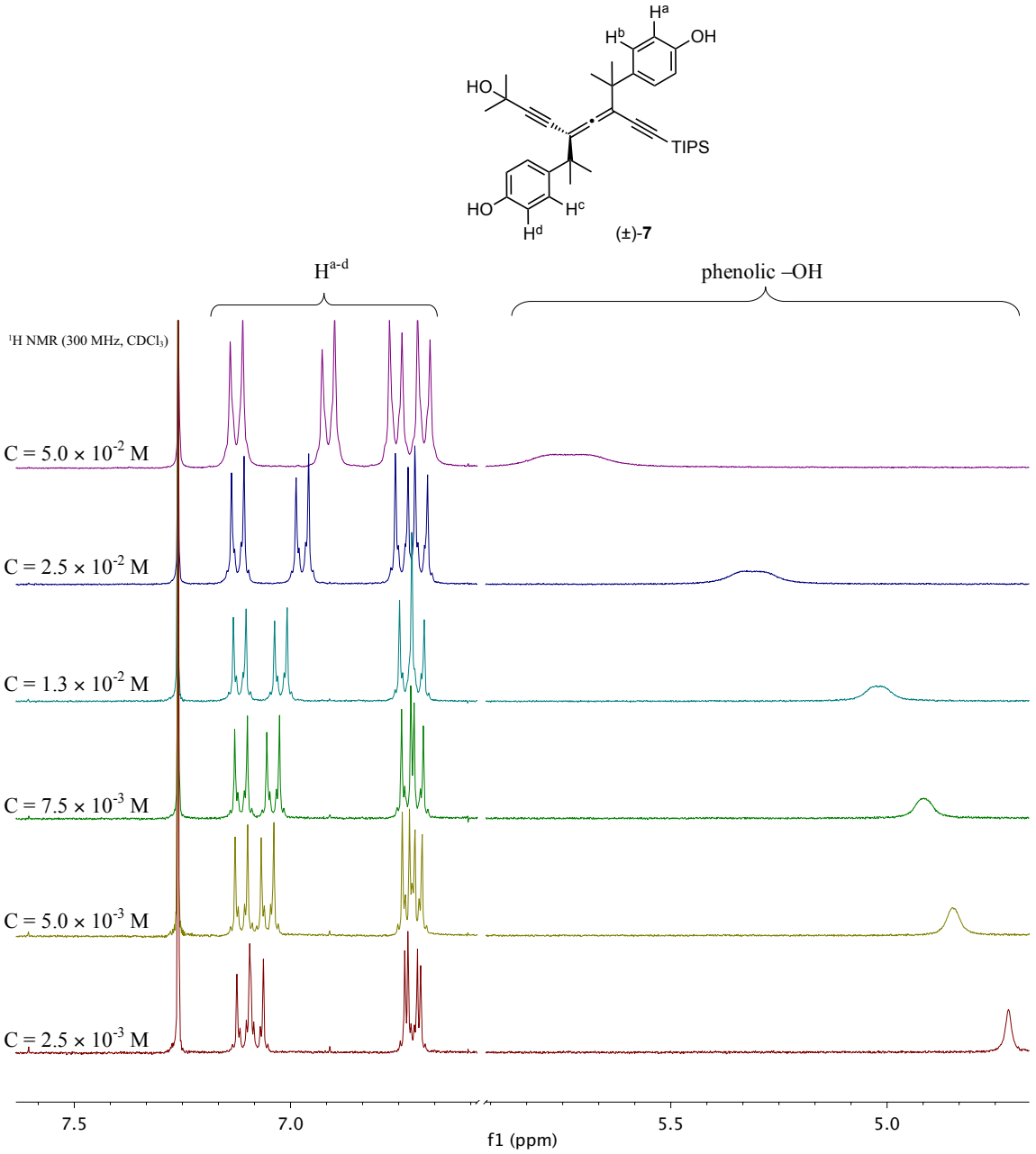

Figure S2. Concentration-dependent ^{1}H NMR spectra of (±)-**7** recorded in $CDCl_3$ at 25 ºC.

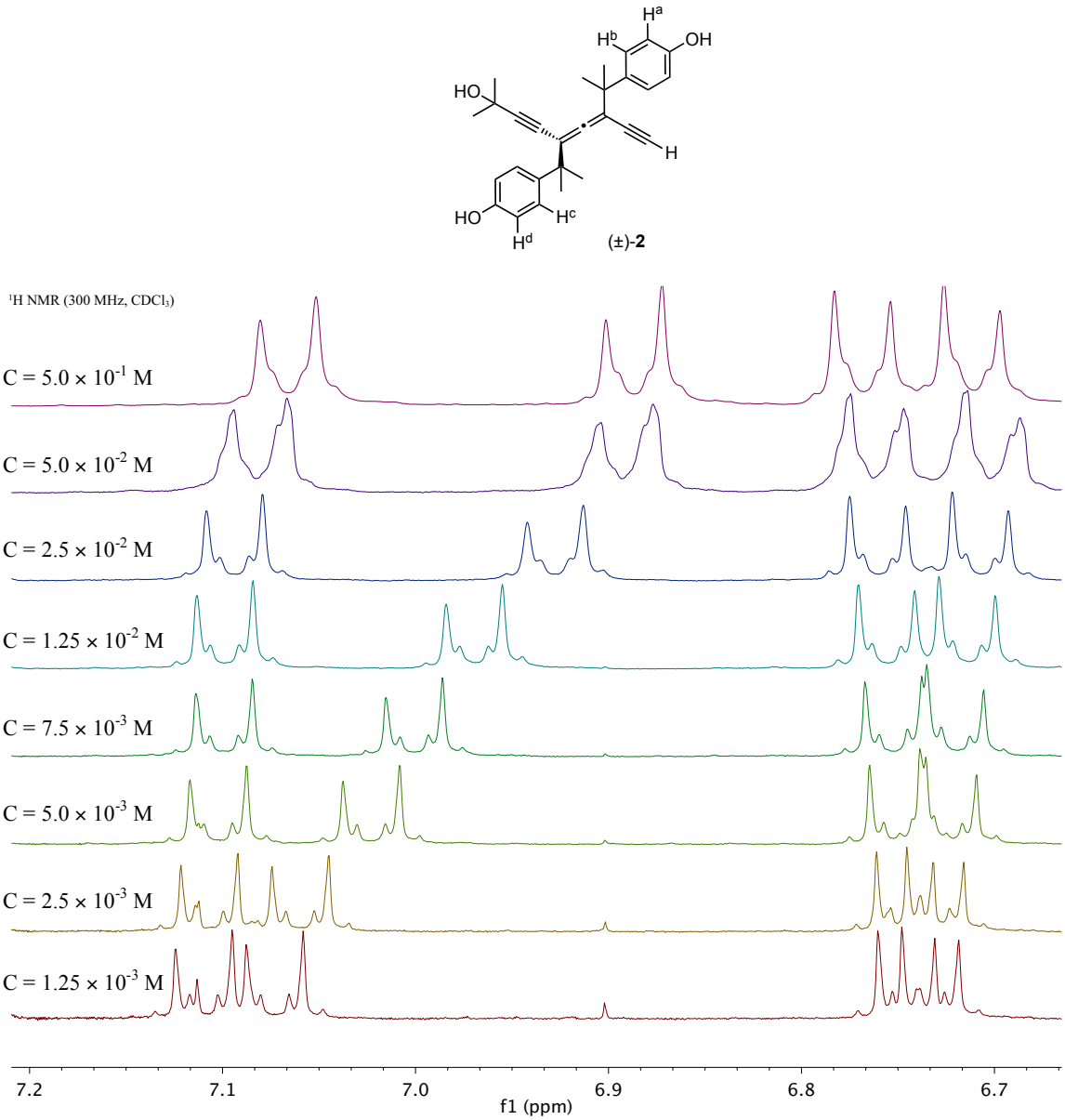

Figure S3. Concentration-dependent ^{1}H NMR spectra of (±)-**2** recorded in $CDCl_3$ (in the presence of ca. 0.2% acetone) at 25 ºC. The OH peaks are not shown for the sake of clarity; there is intense line broadening accompanied by significant downfield shift with increasing concentration.

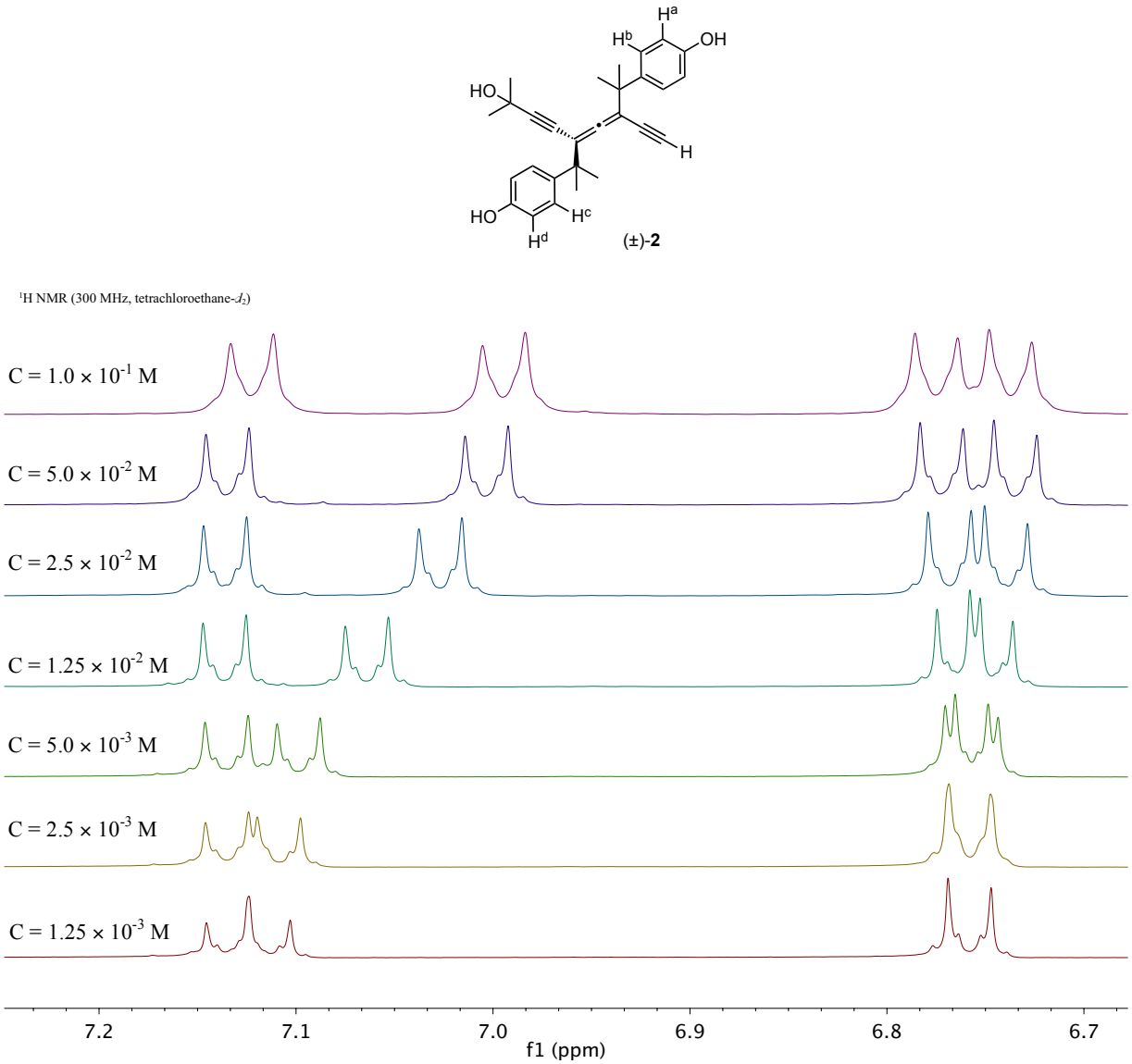

Figure S4. Concentration-dependent ^{1}H NMR spectra of (±)-**2** recorded in 1,1,2,2-tetrachloroethane-d_2 at 25 ºC. The OH peaks are not shown for the sake of clarity.

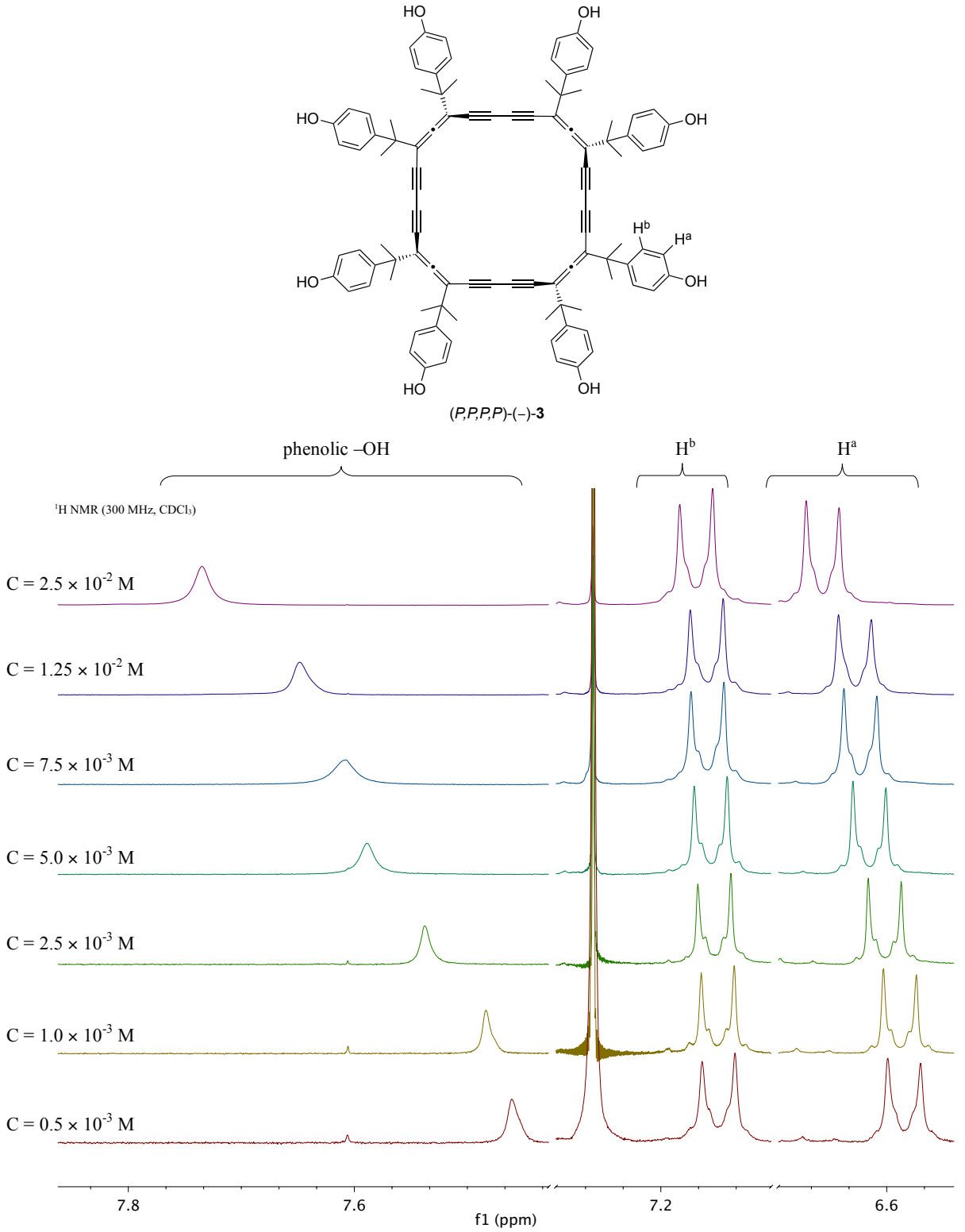

Figure S5. Concentration-dependent ^{1}H NMR spectra of (*P,P,P,P*)-(–)-**3** recorded in $CDCl_3$ (in the presence of 0.4% acetone) at 25 ºC.

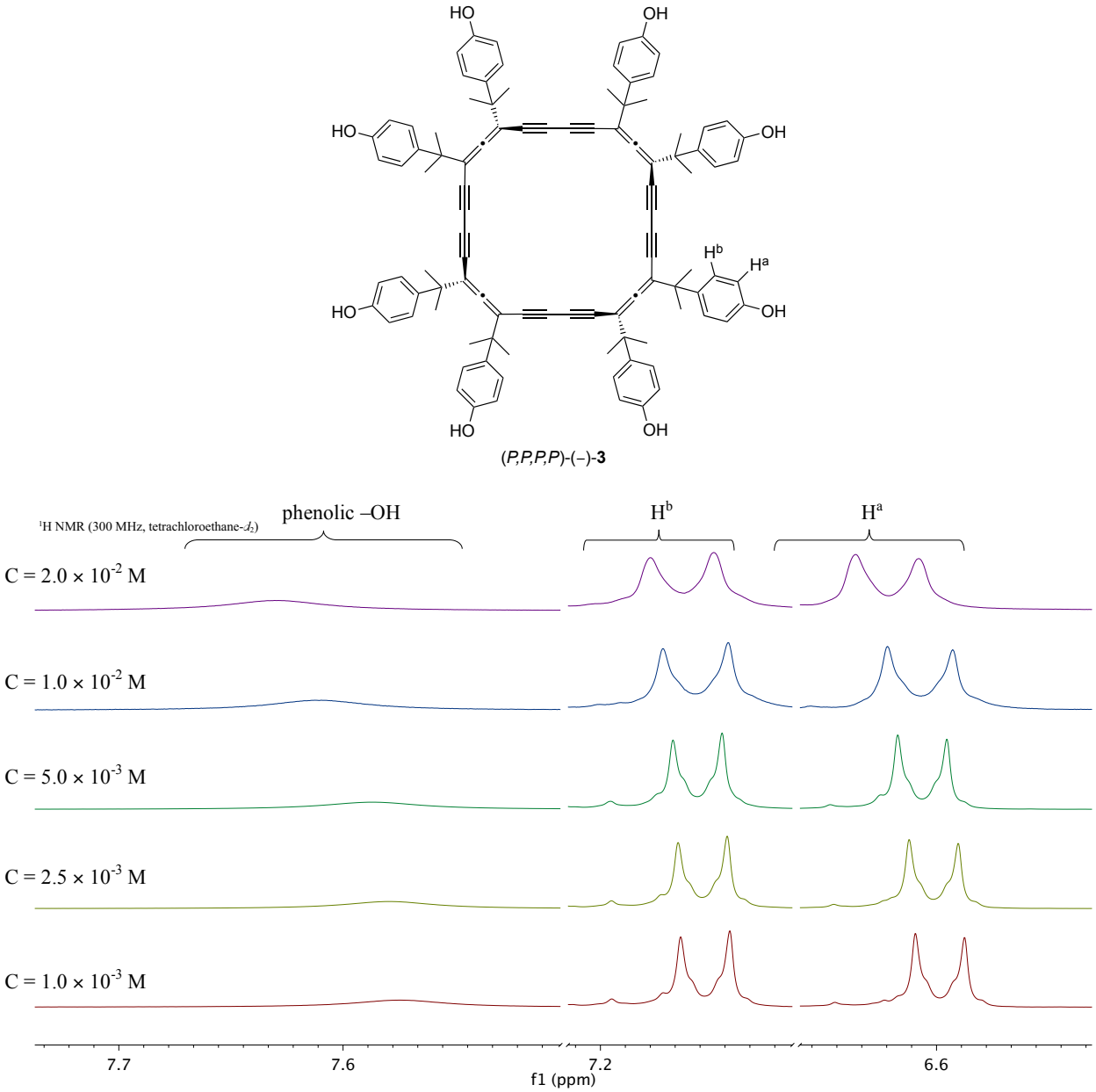

Figure S6. Concentration-dependent ^{1}H NMR spectra of (*P,P,P,P*)-(–)-**3** recorded in 1,1,2,2-tetrachloroethane-d_2 at 25 ºC.

5. Single Crystal X-Ray Analysis of (*M*)-(–)-2 and (*P*,*P*,*P*,*P*)-(–)-3

5.1. General Information

Crystals of compounds (*M*)-(–)-**2** and (*P*,*P*,*P*,*P*)-(–)-**3** were measured on a Bruker Kappa Apex II Duo equipped with a mirror optics monochromator and a Cu microfocus tube (λ = 1.54178 Å) at 100 K. The structures were solved by direct methods with SHELXS-97[3] and refined by full-matrix least-squares analysis (SHELXL-97),[3] using an isotropic extinction correction. CCDC-926014 ((*M*)-(–)-**2**) and CCDC-926015 ((*P,P,P,P*)-(–)-**3**) contain the supplementary crystallographic data for this paper. These data can be obtained free of charge from The Cambridge Crystallographic Data Centre, 12 Union Road, Cambridge CB2 1EZ, UK (Tel.: +44 1223 336 408; Fax: +44 1223 336 033; E-mail: deposit@ccdc.cam.ac.uk), or via www.ccdc.cam.ac.uk/data_request/cif

5.2. X-Ray Crystal Structure of (*M*)-(–)-2 (CCDC-926014)

Single crystals were obtained by slow evaporation of a solution of (*M*)-(–)-**2** in acetone/heptane at 25 °C. The absolute structure of (*M*)-(–)-**2** was known from other physical measurements (i.e. circular dichroism and optical rotation; see section 3).

Table S1. Crystal data and selected details of the data collection and refinement calculations of (*M*)-(–)-**2**.

Sample and crystal data	
CCDC number	926014
Empirical formula	$C_{28}H_{30}O_3$
Formula weight (M_r)	414.52
Temperature	100(2) K
Wavelength	1.54178 Å
Crystal system, space group	orthorhombic, $P2_12_12_1$
Unit cell dimensions	a = 6.3443(8) Å α = 90°
	b = 18.518(2) Å β = 90°
	c = 19.686(2) Å γ = 90°
Volume	2312.8(5) Å^3
Z, Calculated density	4, 1.190 mg cm^{-3}
Absorption coefficient	0.596 mm^{-1}
F(000)	888
Crystal colour/shape	fluorescent colourless needle
Crystal size	0.010 × 0.070 × 0.160 mm
Data collection	
θ range for data collection	$3.28° < \theta < 50.45°$
Limiting indices	$-3 \le h \le 6$, $-18 \le k \le 17$, $-18 \le l \le 19$
Reflections collected / unique	12081 / 2411 [R_{int} = 0.1423]
Absorption correction	multi-scan
Max. and min. transmission	0.9941 and 0.9106
Solution and refinement	
Refinement method	Full-matrix least-squares on F^2
Data / restraints / parameters	2411 / 0 / 298
Goodness-of-fit on F^2	1.143
Final R indices [$I > 2\sigma(I)$]	R_1 = 0.0482, wR_2 = 0.1070
R indices (all data)	R_1 = 0.0603, wR_2 = 0.1121
Flack parameter	0.2(4)
Largest diff. peak and hole	0.235 and –0.247 e Å^{-3}

(a)

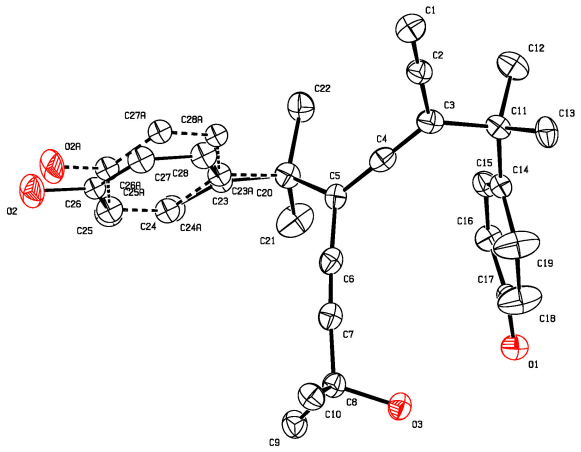

(b)

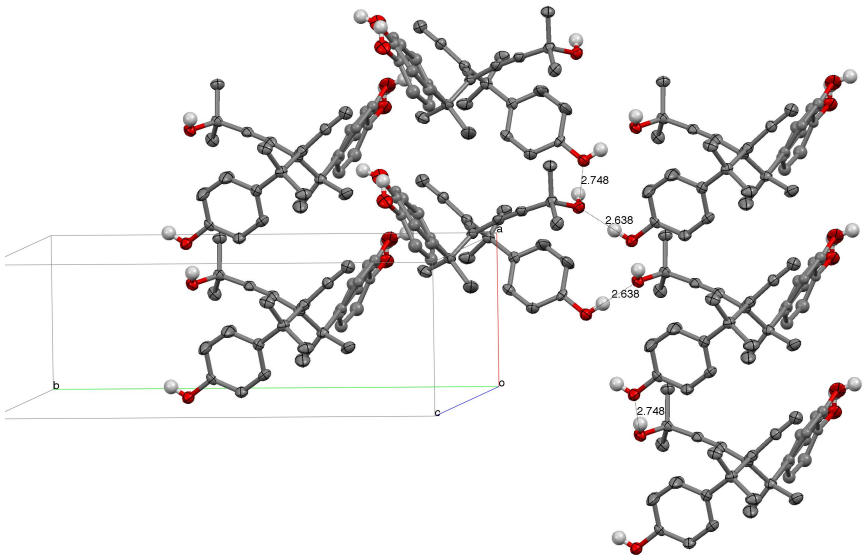

Figure S7. (a) ORTEP plot of (*M*)-(–)-**2**. Arbitrary numbering. Atomic displacement parameters obtained at 100 K are drawn at 50% probability level. H-atoms are omitted for clarity. Selected bond lengths (Å), angles (°) and torsional angles (°): C1–C2: 1.187(5), C2–C3: 1.428(6), C3–C4: 1.310(5), C4–C5: 1.322(5), C5–C6: 1.439(5), C5–C20: 1.529(5), C6–C7: 1.199(5), C3–C4–C5: 176.0(4), C2–C3–C5–C6: –103.6(4), C2–C3–C5–C20: 80.9(4). (b) Arrangement of neighbouring molecules in the crystal packing of (*M*)-(–)-**2** shows that adjacent molecules interact *via* H-bond interactions (O···O distances are given in Å). O2–H was found to take no part in the H-bonding pattern in the crystal. The s.u. values for the O···O separations are 0.003 Å. Hydrogen atoms not involved in the interactions are omitted for clarity. Colour code: red = O, grey = C, white = H.

5.3. X-Ray Crystal Structure of (*P,P,P,P*)-(–)-3 (CCDC-926015)

Single crystals were obtained by slow evaporation of a solution of (*P,P,P,P*)-(–)-**3** in CH_2Cl_2/*n*-heptane (1:1) at 25 °C. $(P)_4$-**3** has crystallographically imposed twofold symmetry. The C_7H_{16} and CH_2Cl_2 components are also disposed about twofold axes.

The C_2-symmetric conformer found in the crystal lattice of $(P)_4$-**3** is similar to that found previously in the crystal structure of the *tert*-butyl-substituted macrocyclic analogue.[4] However, unlike this study,[4] this was the only conformer found in the crystal lattice of $(P)_4$-**3**, without concomitant formation of a D_4-symmetric structure.

The shape-persistent rings in (*P*,*P*,*P*,*P*)-(–)-**3** pack on top of each other without any spatial offset, thus leading to tight, supramolecular columnar stacks with channels parallel to the *b*-axis (Fig. S8). The phenol groups at the periphery of individual macrocycles interact by lateral, intermolecular H-bonds with neighbouring macrocycles of different stacks (Fig. S8b). This mode of packing results in intrinsic porous molecular crystals of (*P*,*P*,*P*,*P*)-(–)-**3**, with solvent-accessible channels propagating indefinitely along the crystallographic *b*-axis (Fig. S8 and S9).

The voids within the crystal structure of (*P*,*P*,*P*,*P*)-(–)-**3** were calculated based on the Solvent Accessible Surface (SAS) by using Mercury 3.0,[5] with a probe sphere radius of 1.2 Å and a grid space of 0.7 Å. The solvent-accessible void volume was determined both in the presence and absence of the guest solvent molecules (*n*-heptane). In the presence of *n*-heptane guest molecules, (*P*,*P*,*P*,*P*)-(–)-**3** exhibits a negligible residual potential solvent-accessible void of 0.63 $Å^3$ per unit cell volume (0.013% of the total unit cell volume). On the other hand, upon removal of the entrapped guest molecules (*n*-heptane), the total potential solvent void volume was calculated as 318.8 $Å^3$ per unit cell (6.5% of the total unit cell volume) (Fig. S9).

When crystals of (*P*,*P*,*P*,*P*)-(–)-**3** are removed from the solvent, the crystallinity is lost within several hours.

Table S2. Crystal data and selected details of the data collection and refinement calculations of (*P,P,P,P*)-(–)-**3**·C_7H_{16}·CH_2Cl_2

Sample and crystal data		
CCDC number	926015	
Empirical formula	$C_{108}H_{106}Cl_2O_8$	
Formula weight	1602.83	
Temperature	100(2) K	
Wavelength	1.54178 Å	
Crystal system, space group	Monoclinic, C_2	
Unit cell dimensions	a = 27.930(3) Å	α = 90°
	b = 8.9770(9) Å	β = 111.190(6)°
	c = 20.9383(15) Å	γ = 90°
Volume	4894.9(8) Å^3	
Z, Calculated density	2, 1.088 mg cm^{-3}	
Absorption coefficient	1.009 mm^{-1}	
F(000)	1704	
Crystal colour/shape	clear pale yellow rod	
Crystal size	0.02 × 0.08 × 0.12 mm	
Data collection		
θ range for data collection	2.26° < θ < 50.08°	
Limiting indices	$-26 \le h \le 27$, $-8 \le k \le 6$, $-20 \le l \le 11$	
Reflections collected / unique	9424 / 2706 [R_{int} = 0.0339]	
Absorption correction	multi-scan	
Max. and min. transmission	0.7499 and 0.5764	
Solution and refinement		
Refinement method	Full-matrix least-squares on F^2	
Data / restraints / parameters	2706 / 14 / 546	
Goodness-of-fit on F^2	1.408	
Final R indices [$I > 2\sigma(I)$]	R_1 = 0.1055, wR_2 = 0.2781	
R indices (all data)	R_1 = 0.1131, wR_2 = 0.2893	
Flack parameter	0.1(2)	
Largest diff. peak and hole	0.560 and –0.342 e Å^{-3}	

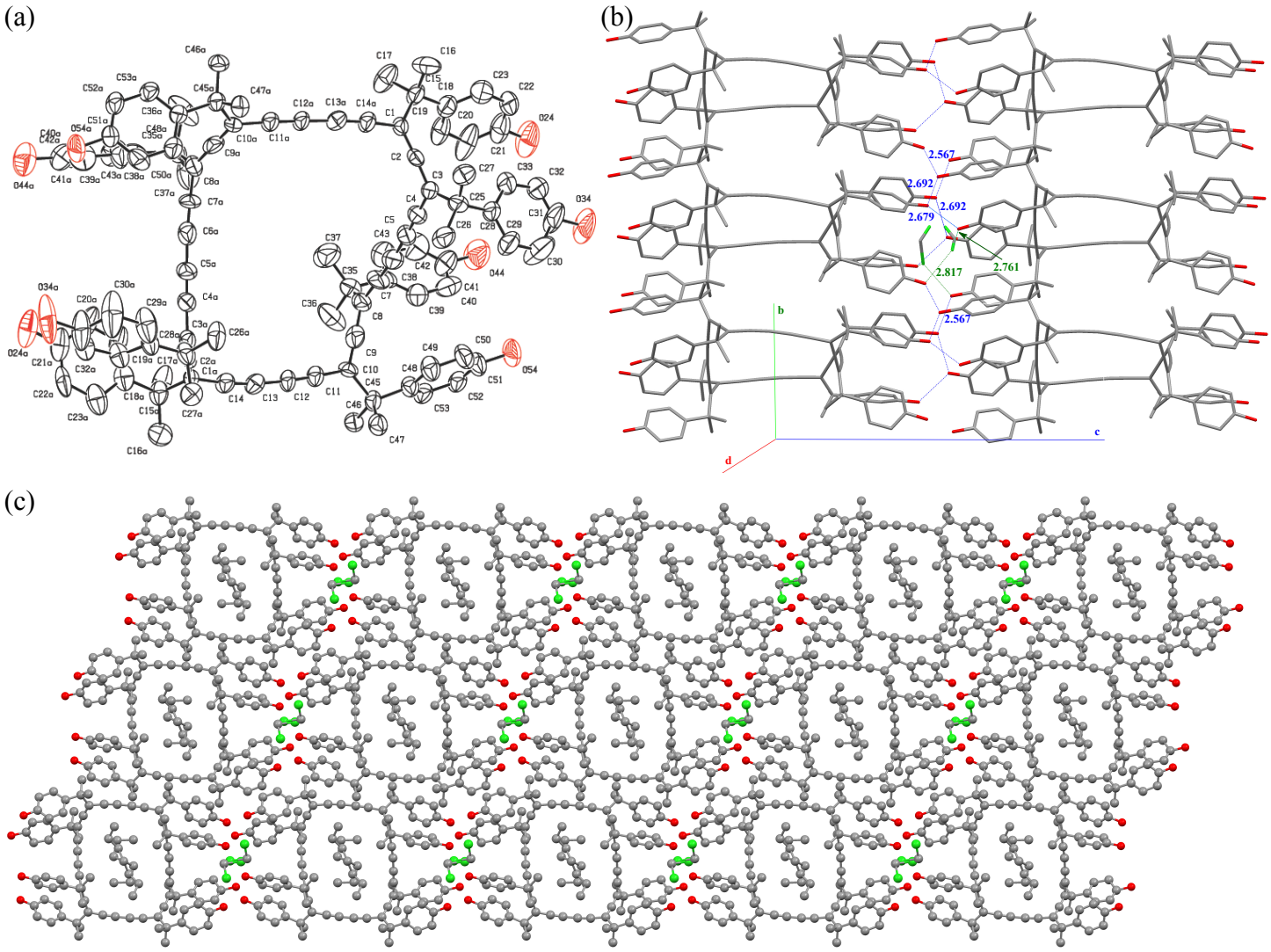

Figure S8. (a) ORTEP plot of (*P*,*P*,*P*,*P*)-(–)-**3**. Arbitrary numbering. The labels of atoms generated by crystallographic twofold axis (–x, y, 2–z) are labeled with an additional "a". Atomic displacement parameters obtained at 100 K are drawn at 50% probability level. Selected bond lengths (Å), angles (°) and torsional angles (°): C1–C2: 1.293(10), C2–C3: 1.337(11), C3–C4: 1.430(13), C4–C5: 1.176(12), C2–C3–C4: 116.3(8), C9a–C10a–C1–C2: –63.5(8). (b) Arrangement of neighbouring molecules in the crystal packing of (*P*,*P*,*P*,*P*)-(–)-**3** shows the formation of columnar stacks by axial packing of macrocycles; individual molecules interact *via* lateral H-bonds (highlighted with blue dotted lines) with molecules of neighbouring stacks, thus leading to further assembly of the columnar stacks into a microporous structure. Dichloromethane molecules are also incorporated in the crystal and participate in two O–H···Cl interactions (highlighted with green dotted lines). O···O and Cl···O distances are shown in Å. (c) Microporous architecture with *n*-heptane molecules located inside each channel viewed along the *b*-axis. Hydrogen atoms are omitted for clarity. Colour code: green = Cl, red = O, grey = C.

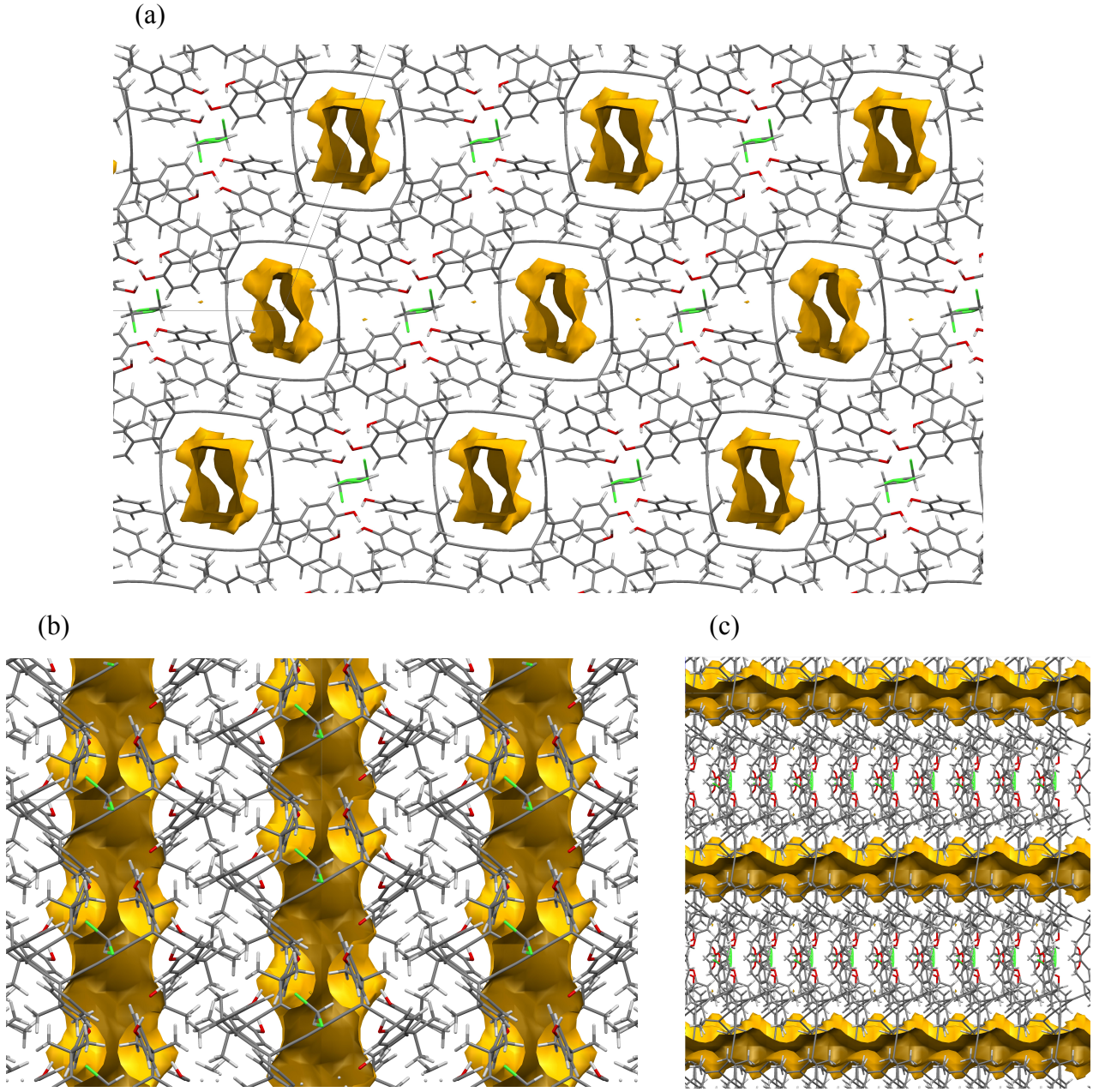

Figure S9. Representation of the solvent-accessible channels in the crystal structure of (*P*,*P*,*P*,*P*)-(–)-**3** viewed along the (a) *b*, (b) *c* and (c) *a* axis, with guest solvent (*n*-heptane) omitted. The solvent-accessible channels (voids) are shown in yellow, demonstrating that this structure is formally porous to solvents. Colour code: green = Cl, red = O, grey = C, white = H.

6. Circular Dichroism (CD) and UV/Vis Spectra of Compounds 2, 3 and 9–11

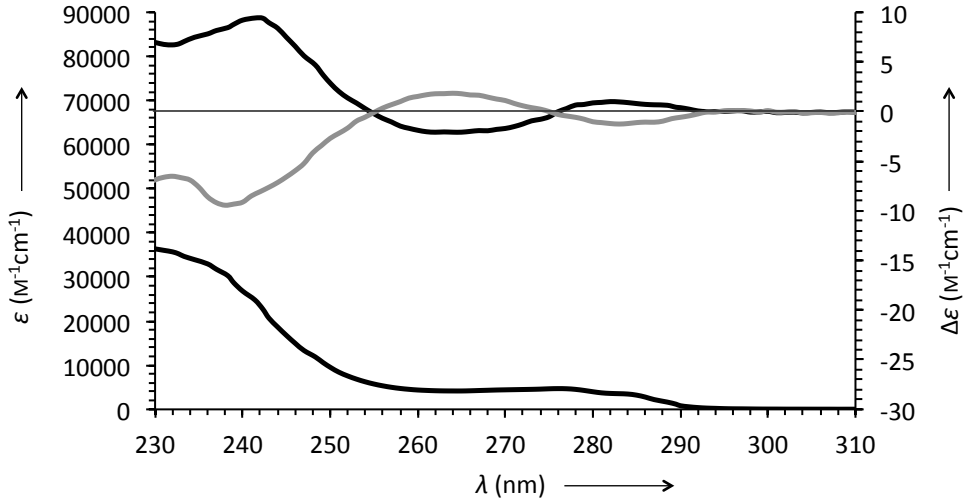

Figure S10. Top: CD spectra of enantiopure (*P*)-(+)-**2** (black line) and enantiopure (*M*)-(–)-**2** (grey line). Bottom: UV/Vis spectrum. All spectra were measured in CH_3CN at 25 °C.

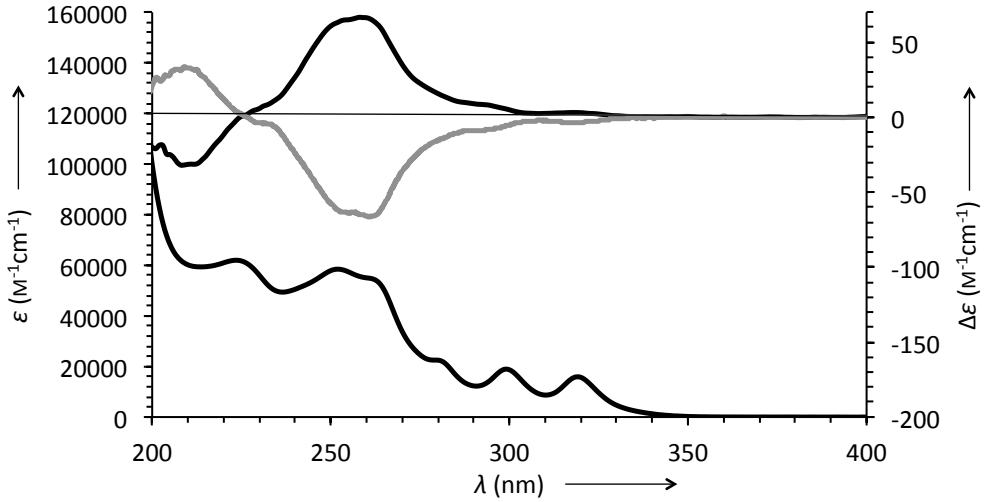

Figure S11. Top: CD spectra of enantiopure (*P,P*)-(+)-**9** (black line) and enantiopure (*M,M*)-(–)-**9** (grey line). Bottom: UV/Vis spectrum. All spectra were measured in CH_3CN at 25 °C.

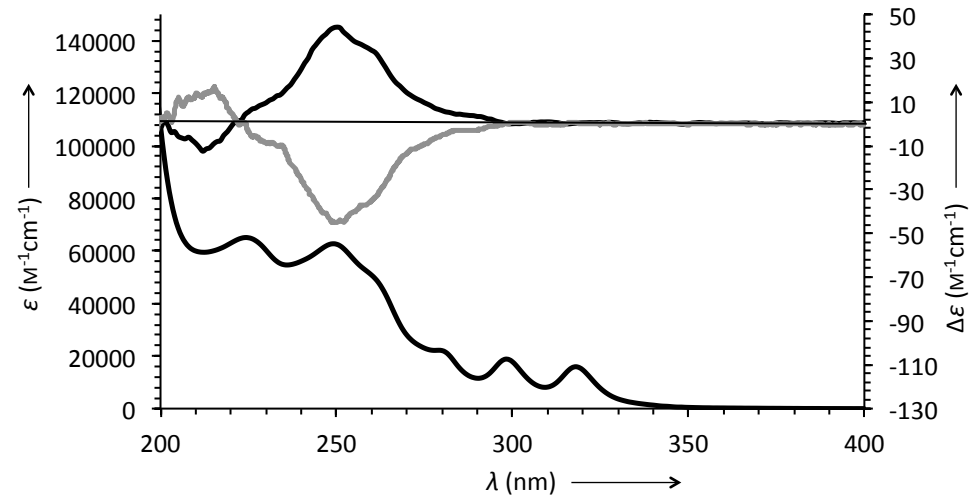

Figure S12. Top: CD spectra of enantiopure (*P,P*)-(+)-**10** (black line) and enantiopure (*M,M*)-(–)-**10** (grey line). Bottom: UV/Vis spectrum. All spectra were measured in CH_3CN at 25 °C.

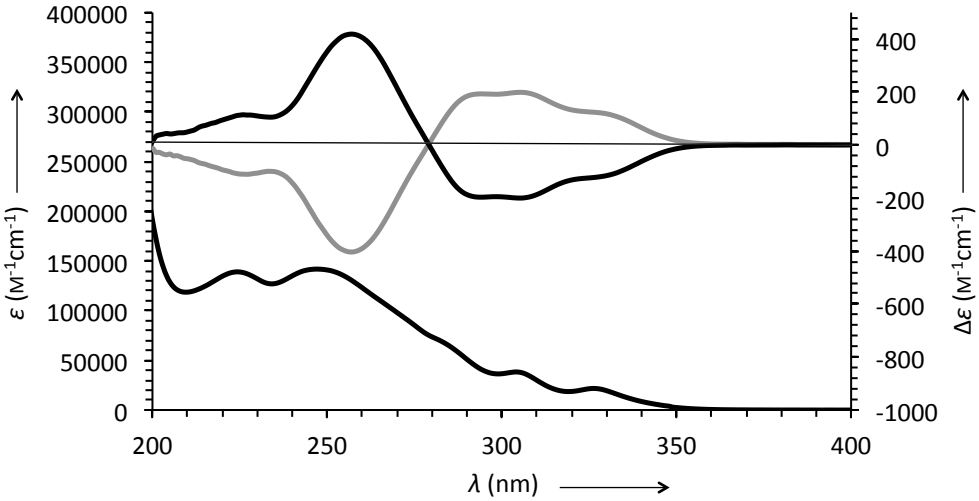

Figure S13. Top: CD spectra of enantiopure (*P,P,P,P*)-(–)-**11** (black line) and enantiopure (*M,M,M,M*)-(+)-**11** (grey line). Bottom: UV/Vis spectrum. All spectra were measured in CH_3CN at 25 °C.

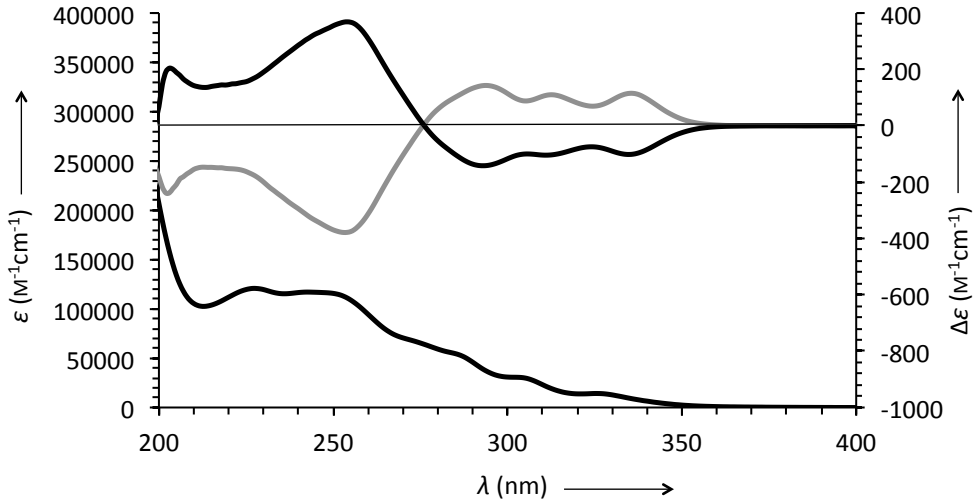

Figure S14. Top: CD spectra of enantiopure (*P,P,P,P*)-(–)-**3** (black line) and enantiopure (*M,M,M,M*)-(+)-**3** (grey line). Bottom: UV/Vis spectrum. All spectra were measured in CH_3CN at 25 °C.

The g-factor plot for (*P,P,P,P*)-(–)-**3** was also analysed (Fig. S15). The g-factor is defined as the ratio between the molar circular dichroism $\Delta\varepsilon$ and the molar extinction coefficient ε ($g = \Delta\varepsilon/\varepsilon$), and can be used to estimate the relative contributions of electric and magnetic transition dipole moments to the Cotton effects. In the case of (*P,P,P,P*)-(–)-**3** – and similar to our previous studies concerning the corresponding non-laterally-functionalised macrocyclic analogue[6] – the larger g-values between 310 nm and 370 nm clearly indicate stronger magnetic dipole contributions, while the opposite is evident with regard to the Cotton effects around 255 nm.

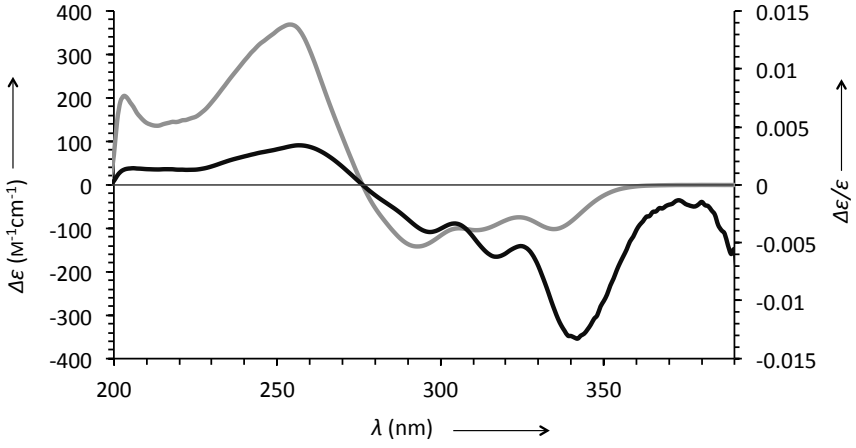

Figure S15. CD spectrum (grey line) and g-factor plot (black line) for (*P,P,P,P*)-(–)-**3**. UV/Vis and CD spectra were measured in CH_3CN at 25 °C.

6.1. Comparison Between the ECD Spectra of Compounds 2, 3, 10, and S1–S3

Comparison between the ECD spectra of the *tert*-butyl-substituted monomer **S1**[2,7] and the corresponding phenol-substituted monomer **2** shows similar values for their CD response. On the other hand, the *tert*-butyl-substituted dimer **S2**[6,7] and the tetrameric macrocycle **S3**,[4,6] exhibit substantially higher values as compared to the corresponding values obtained for the phenol-substituted analogues **10** and **3**, respectively (Fig. S16).

Although the ECD spectra in Fig. S16 were recorded in different solvents (*n*-hexane for **S1**–**S3** and CH_3CN for **2**, **10** and **3**), the difference in $\Delta\varepsilon$ values observed should not be ascribed to solvent effect, since previous studies showed that the CD spectra are nearly independent of solvent polarity (i.e. from *n*-hexane to MeOH).[7] It should be rather ascribed to electronic effects (lowering of the molar extinction coefficients).

To probe further the effect of the electronic properties on lowering the $\Delta\varepsilon$ values, we compared the extinction coefficient (ε) and g-factor ($\Delta\varepsilon/\varepsilon$) values of the phenol-substituted macrocycle **3** and the *tert*-butyl-substituted macrocycle **S3** (Fig. S17). The g-factor values of **3** and **S3**[6] at the region of interest (around 250 nm) are almost the same (0.033–0.034) which means that the magnetic transition dipole moment in both macrocycles are very similar (Fig. S17, left). This behaviour points towards very similar conformational stability for the two macrocycles (**3** and **S3**), especially for their alleno-acetylenic backbones from which their CD response originates. On the other hand, these macrocycles exhibit quite different ε values, especially a significant decrease of the ε value in **3** (ε = 116550 $M^{-1}cm^{-1}$, 247 nm, MeCN) compared to **S3** (ε = 210700 $M^{-1}cm^{-1}$, 245 nm, *n*-hexane)[6] (Fig. S17, right). Since the absolute intensity of Cotton effects is proportional to the extinction coefficients, a smaller intensity of the Cotton effect would be expected for **3** compared to **S3**. Indeed, consistent with this hypothesis, the Cotton effect of **3** ($\Delta\varepsilon$ = ± 375 $M^{-1}cm^{-1}$, 254 nm, MeCN) is significantly decreased compared to **S3** ($\Delta\varepsilon$ = ± 790 $M^{-1}cm^{-1}$, 253 nm, *n*-hexane), in an almost linear manner. Similar conclusions can be drawn by comparing the corresponding UV/Vis spectra of dimers **10** (ε = 60940 $M^{-1}cm^{-1}$, 240 nm; $\Delta\varepsilon$ = ± 45 $M^{-1}cm^{-1}$, 252 nm, MeCN) and **S2** (ε = 79313 $M^{-1}cm^{-1}$, 246 nm; $\Delta\varepsilon$ = ± 102 $M^{-1}cm^{-1}$, 246 nm, *n*-hexane).[6]

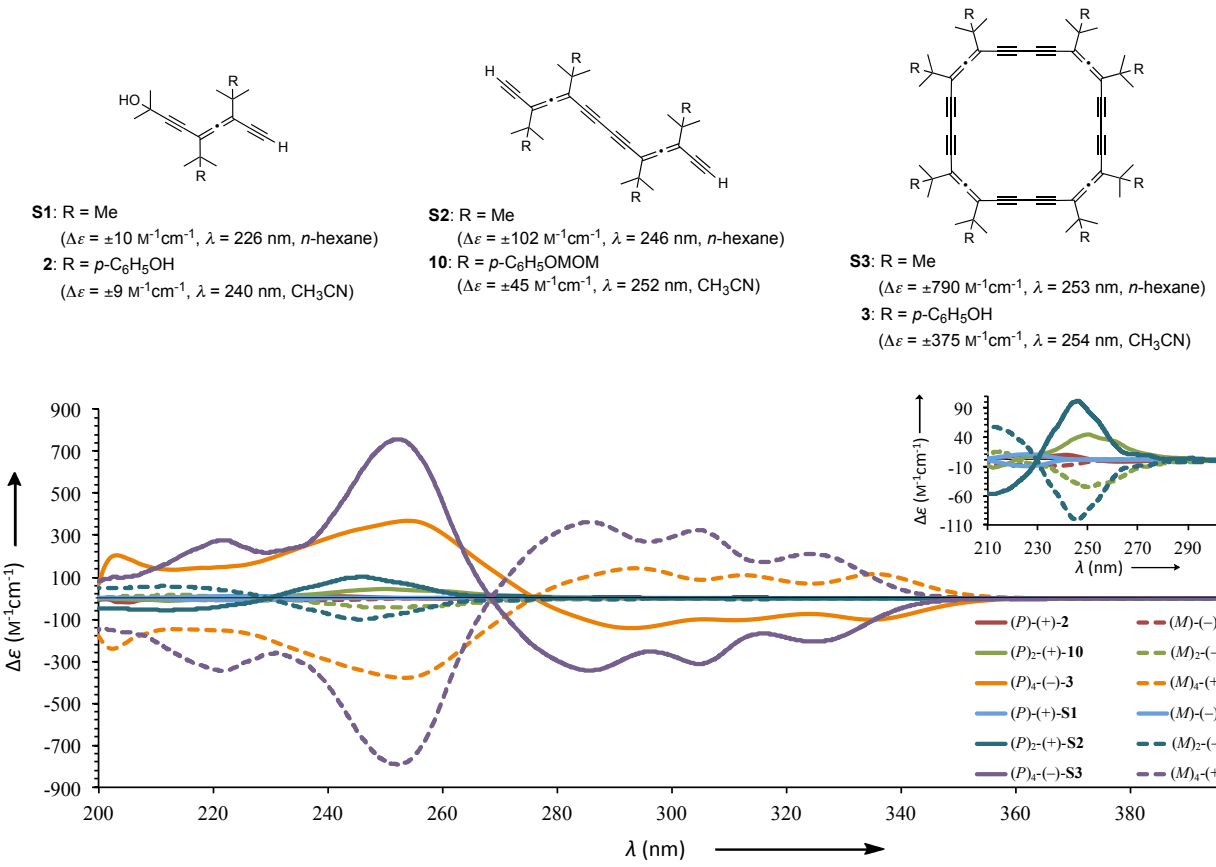

Figure S16. Comparison between the ECD spectra of the *tert*-butyl-substituted compounds used in our previous studies (**S1**, **S2** and **S3**)[2,4,6,7] and the corresponding phenol-substituted compounds studied in the current study (**2**, **10** and **3**). CD spectra for **S1**–**S3** were measured in *n*-hexane, whereas **2**, **10** and **3** were measured in CH_3CN at 25 °C. The inset is an expansion of the region between 210 and 310 nm, for the monomeric (**S1** and **2**) and the dimeric (**S2** and **10**) analogues.

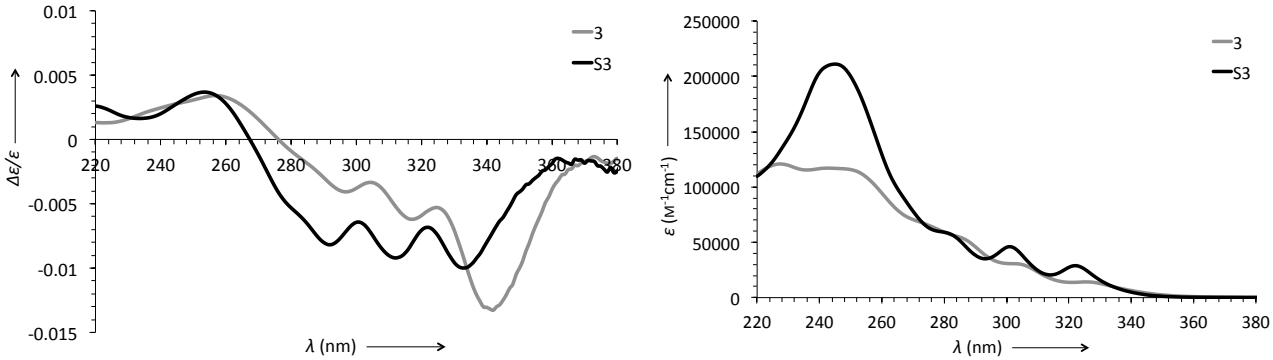

Figure S17. g-Factor plots (left) and UV/Vis spectra (right) of **S3**[6] and **3**. UV/Vis spectrum of **S3** was measured in *n*-hexane, whereas **3** was measured in CH_3CN at 25 °C.

7. Molecular Dynamics Simulations

Molecular dynamics (MD) calculations were performed using the OPLS-2005 force field as implemented in MacroModel 9.7.[8] Equilibration time: 50 ps; Simulation time: 2000 ps; Solvation: Implicit $CHCl_3$ (constant dielectric permittivity); Thermodynamic conditions: 300 K, 1 bar.

These calculations showed a greater conformational flexibility of the lateral phenol groups in **3** as compared to corresponding lateral *t*-butyl groups in **S3** (Fig. S18).[9] However, it should be noted that the conformational flexibility comes only from the phenolic substituents (i.e. the flexibility of the alleno-acetylenic backbone does not increase substantially) and as such, it should have only a minor effect on the chiroptical properties of **3**.

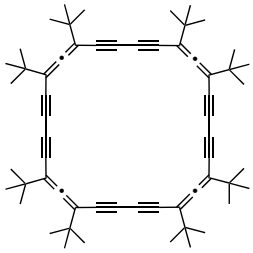

(*P*,*P*,*P*,*P*)/(*M*,*M*,*M*,*M*)-**S3**

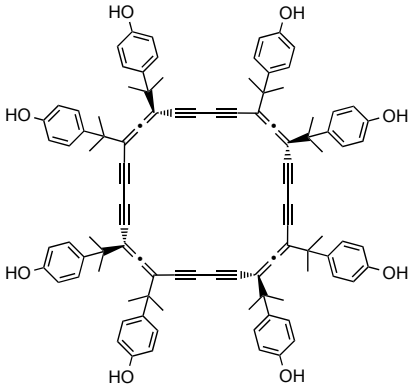

(*M*,*M*,*M*,*M*)-(+)-**3**

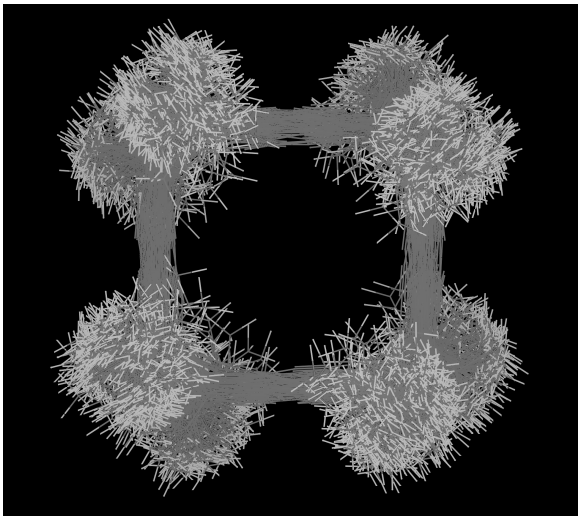

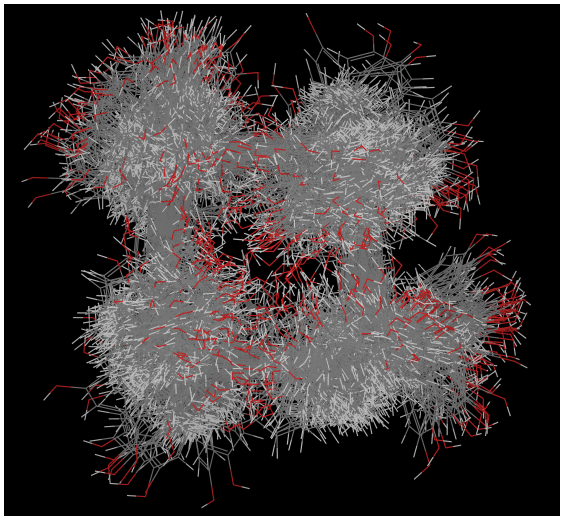

Figure S18. Overlay of 100 structures (for each molecule) obtained from molecular dynamics over a period of 2000 ps. $(M)_4$-(+)-**3** (right) shows much higher conformational flexibility than **S3**[9] (left).

8. Concentration-Dependent ECD Measurements

Concentration-dependent CD measurements were performed for (*P*)-(+)-**2** and $(M)_4$-(+)-**3** in 1,1,2,2-tetrachloroethane at 25 ºC (Fig. S19). Similar to the corresponding NMR measurements (Fig. S2–S6), the use of 1,1,2,2-tetrachloroethane allowed for performing CD studies in the absence of a polar co-solvent, although aggregation was still observed upon storage at rt for several minutes. These measurements showed no amplification of chirality in solution in the concentration range between $5.0 \times 10^{-5} - 2.5 \times 10^{-3}$ for (*P*)-(+)-**2** (Fig. S19, left) and $1.0 \times 10^{-5} - 1.0 \times 10^{-4}$ for $(M)_4$-(+)-**3** (Fig. S19, right). Similar studies in $CDCl_3$ or CH_2Cl_2 (in the presence of a trace amount of a polar co-solvent) gave essentially the same results. Also, as expected by virtue of its high polarity, the use of CH_3CN in these experiments did not alter these results (spectra not shown).

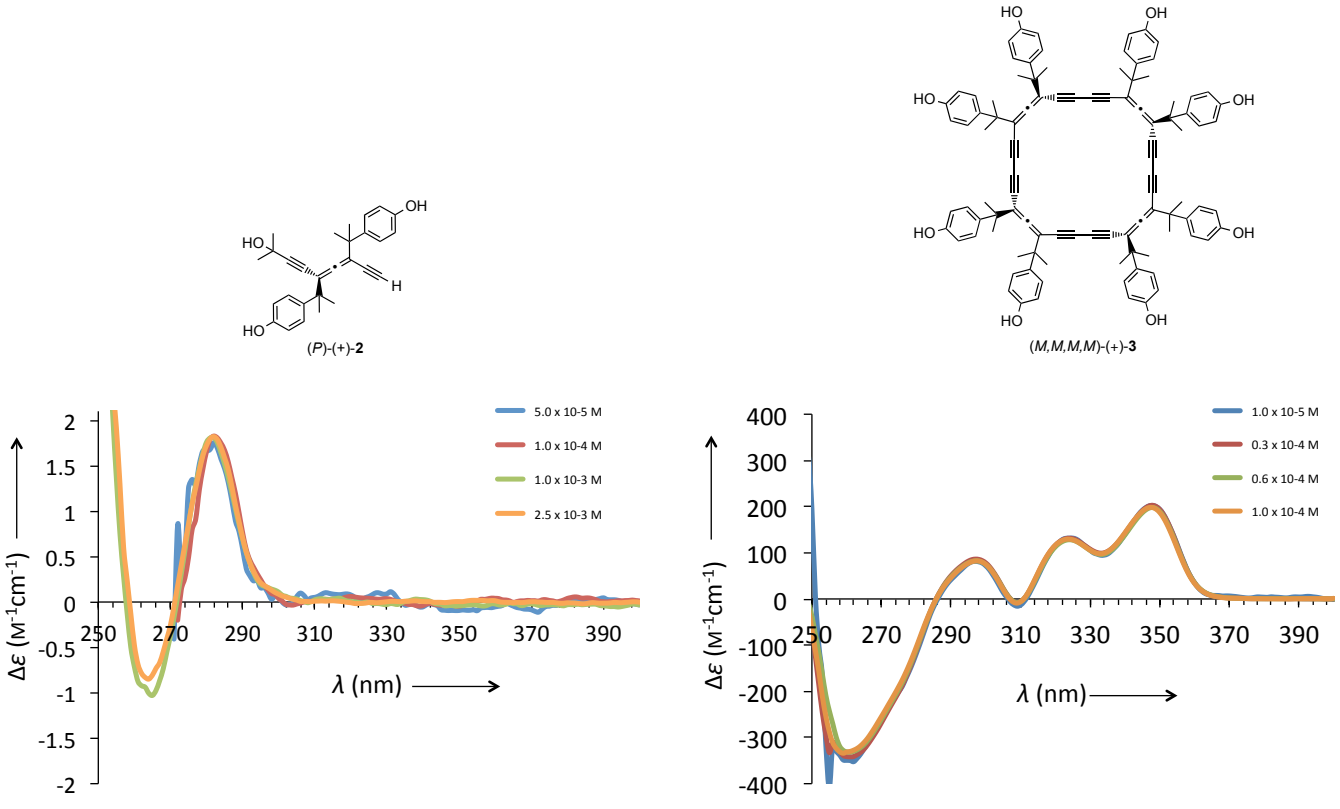

Figure S19. Concentration-dependent ECD spectra of (*P*)-(+)-**2** (left) and $(M)_4$-(+)-**3** (right) recorded in 1,1,2,2-tetrachloroethane at 25 ºC.

9. ^{1}H and ^{13}C NMR Spectra of Compounds 2, 3, 5–7 and 9–11

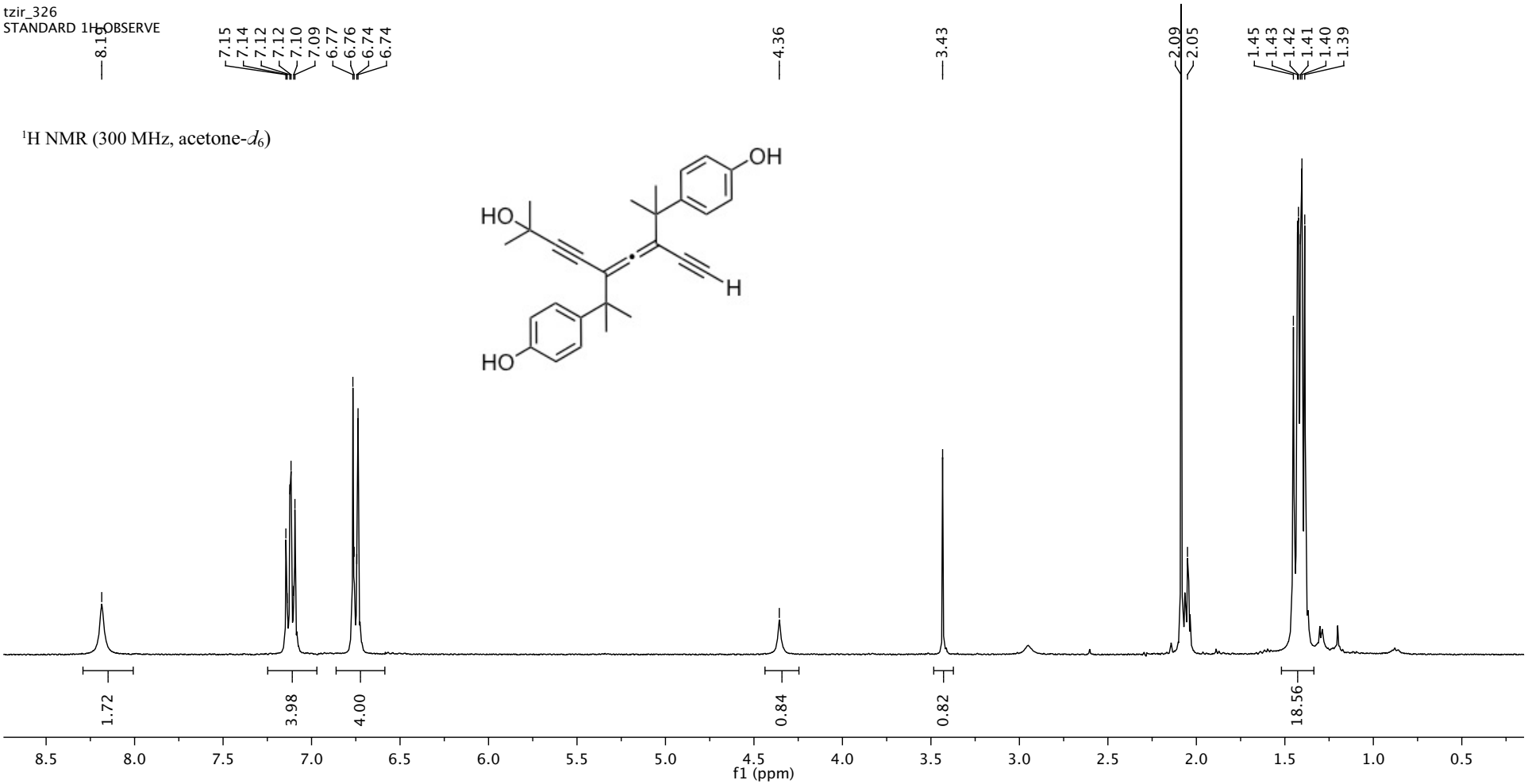

Figure S20. ^{1}H NMR (300 MHz, acetone-d_6, 25 °C) spectrum of compound (±)-**2**.

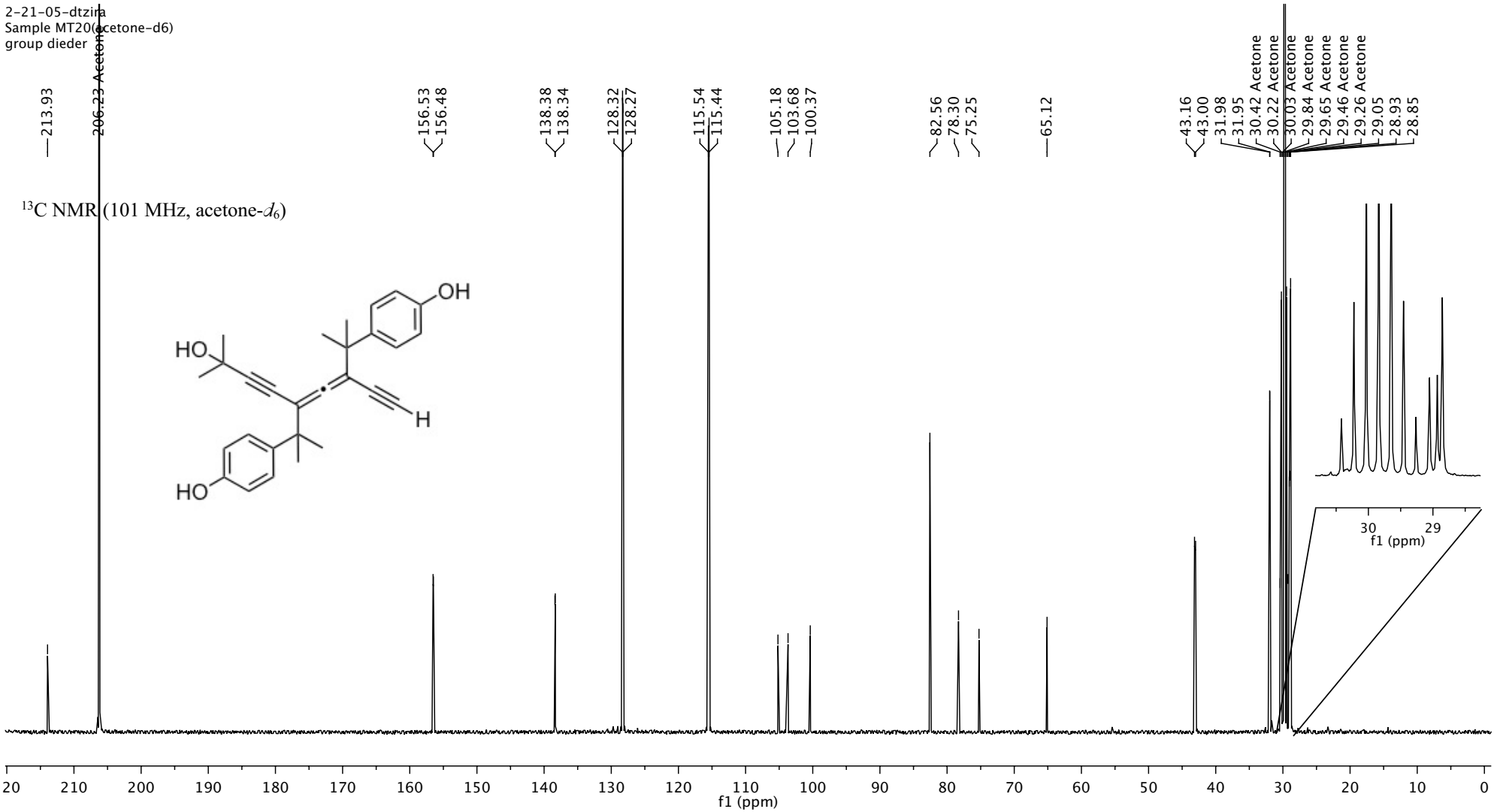

Figure S21. ^{13}C NMR (101 MHz, acetone-d_6, 25 °C) spectrum of compound (±)-**2**.

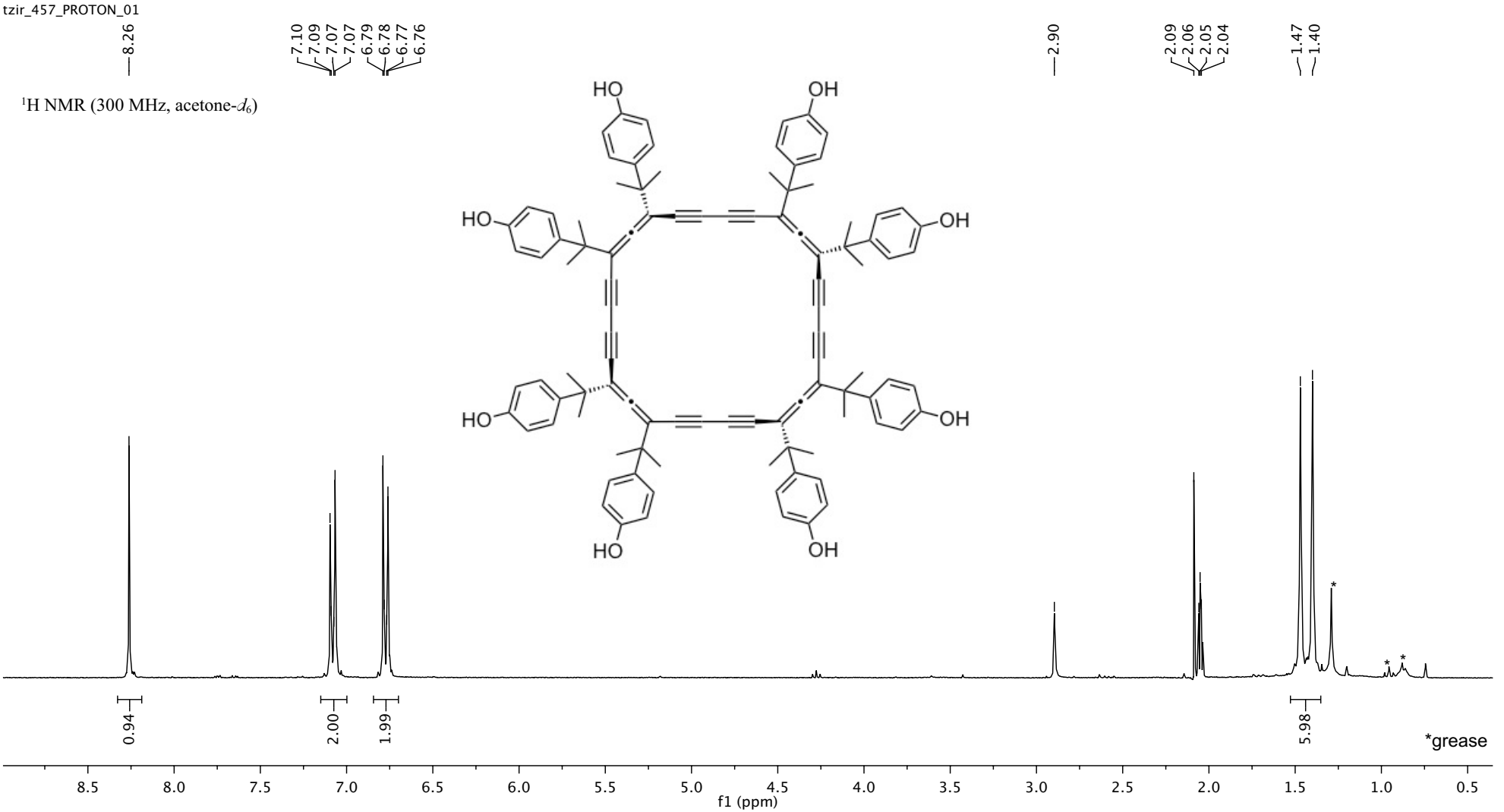

Figure S22. ^{1}H NMR (300 MHz, acetone-d_6, 25 °C) spectrum of compound (*P*,*P*,*P*,*P*)-(–)-**3**.

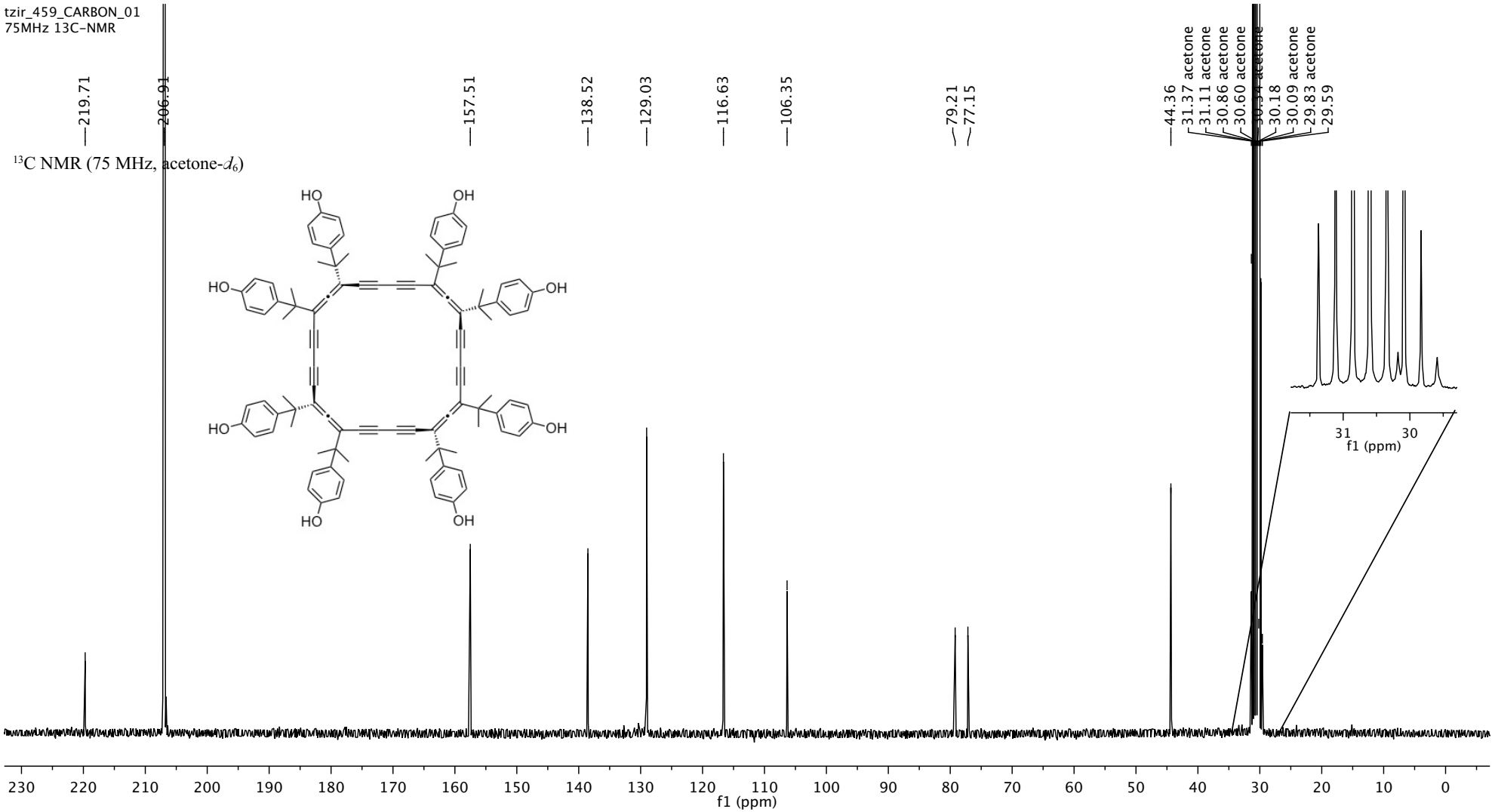

Figure S23. ^{13}C NMR (75 MHz, acetone-d_6, 25 °C) spectrum of compound (*P*,*P*,*P*,*P*)-(–)-**3**.

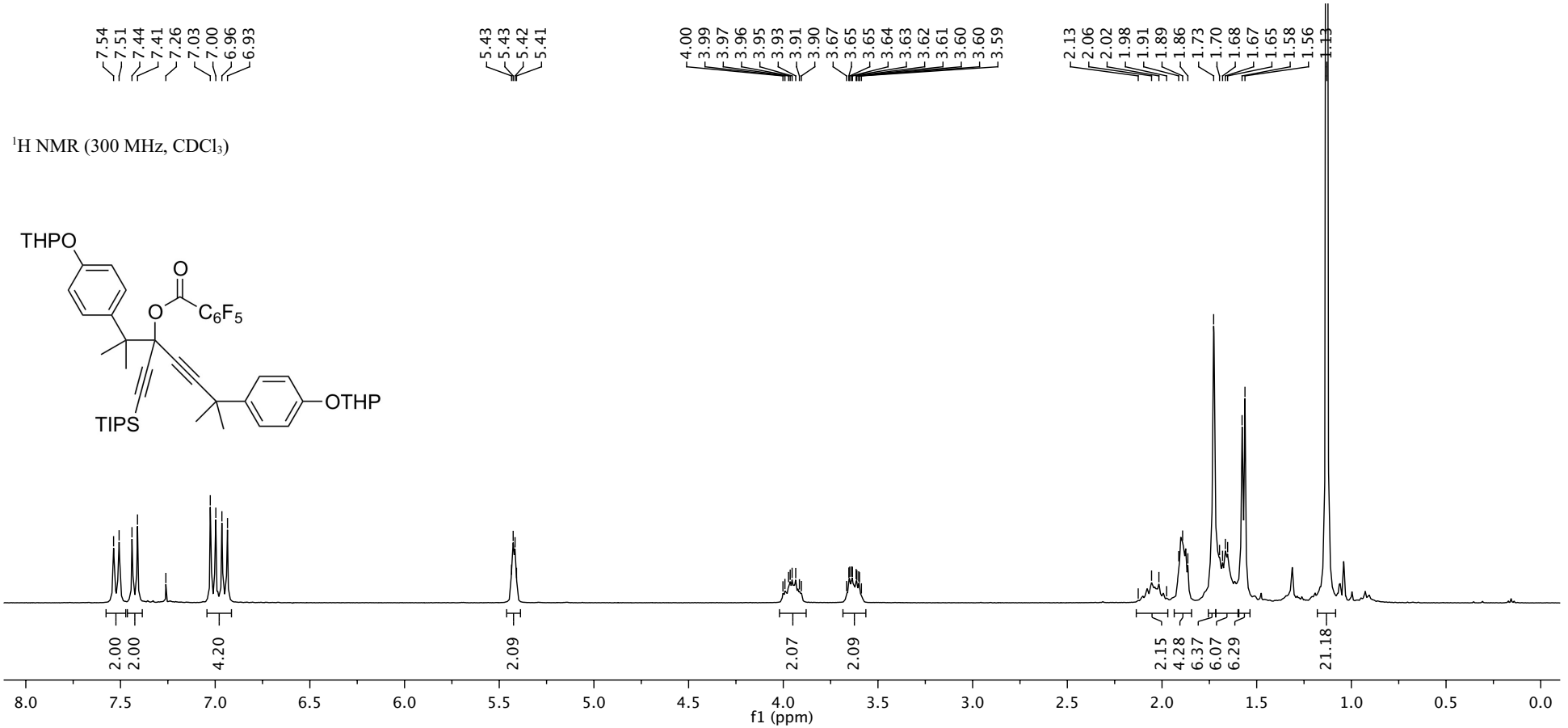

Figure S24. ^{1}H NMR (300 MHz, $CDCl_3$, 25 °C) spectrum of compound **5**.

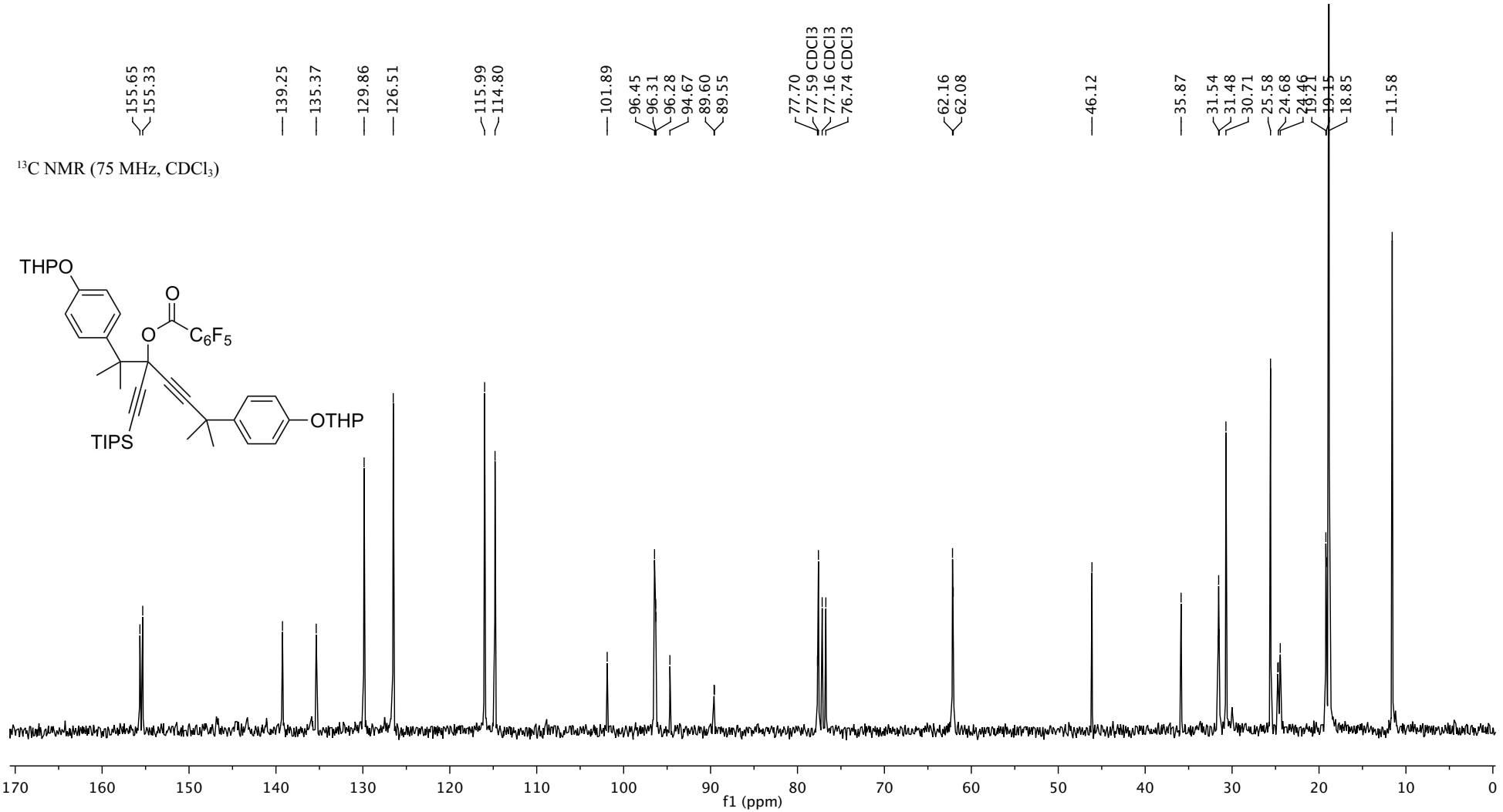

Figure S25. ^{13}C NMR (75 MHz, $CDCl_3$, 25 °C) spectrum of compound **5**.

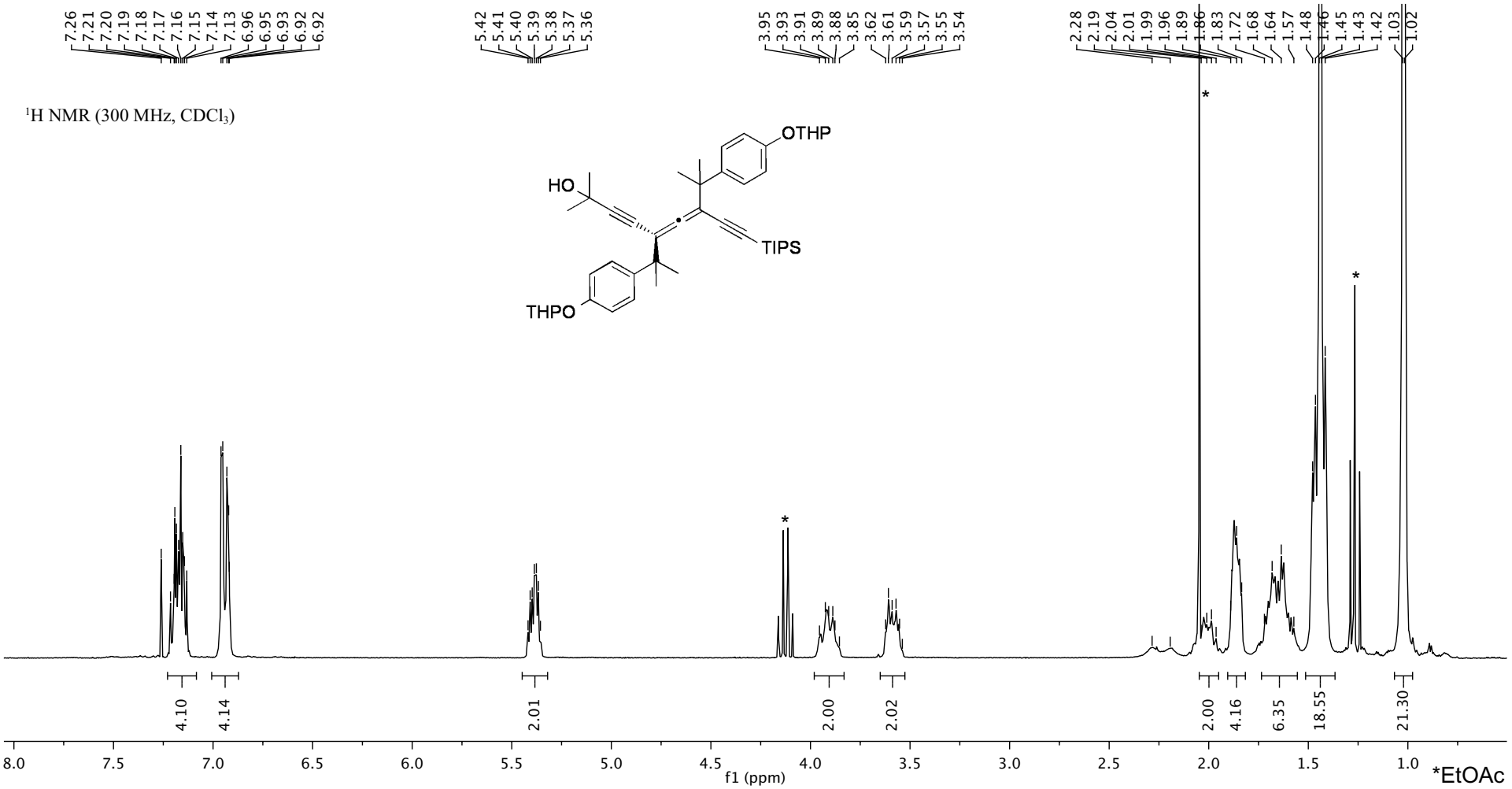

Figure S26. ^{1}H NMR (300 MHz, $CDCl_3$, 25 °C) spectrum of compound **6**.

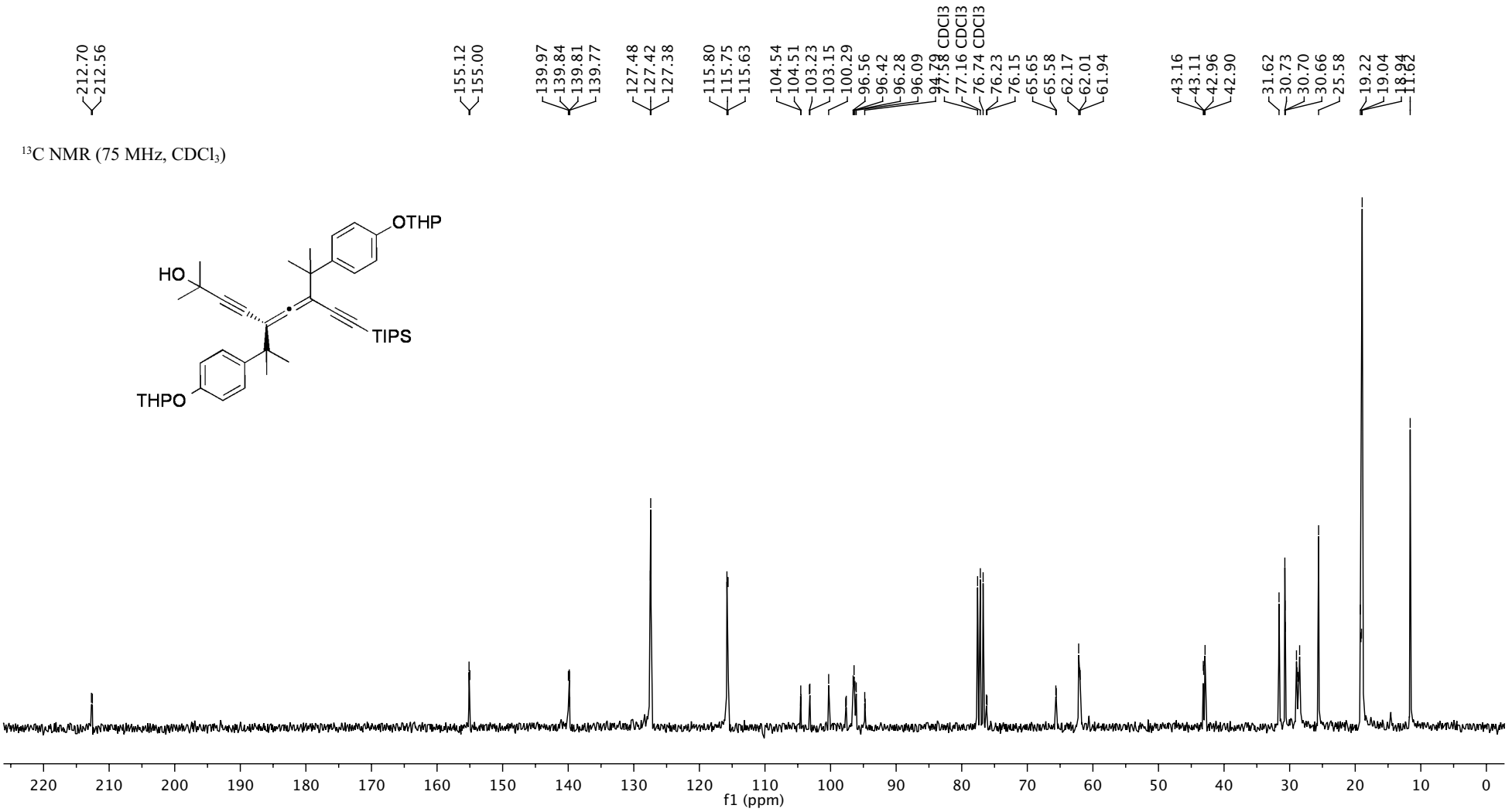

Figure S27. ^{13}C NMR (75 MHz, $CDCl_3$, 25 °C) spectrum of compound **6**.

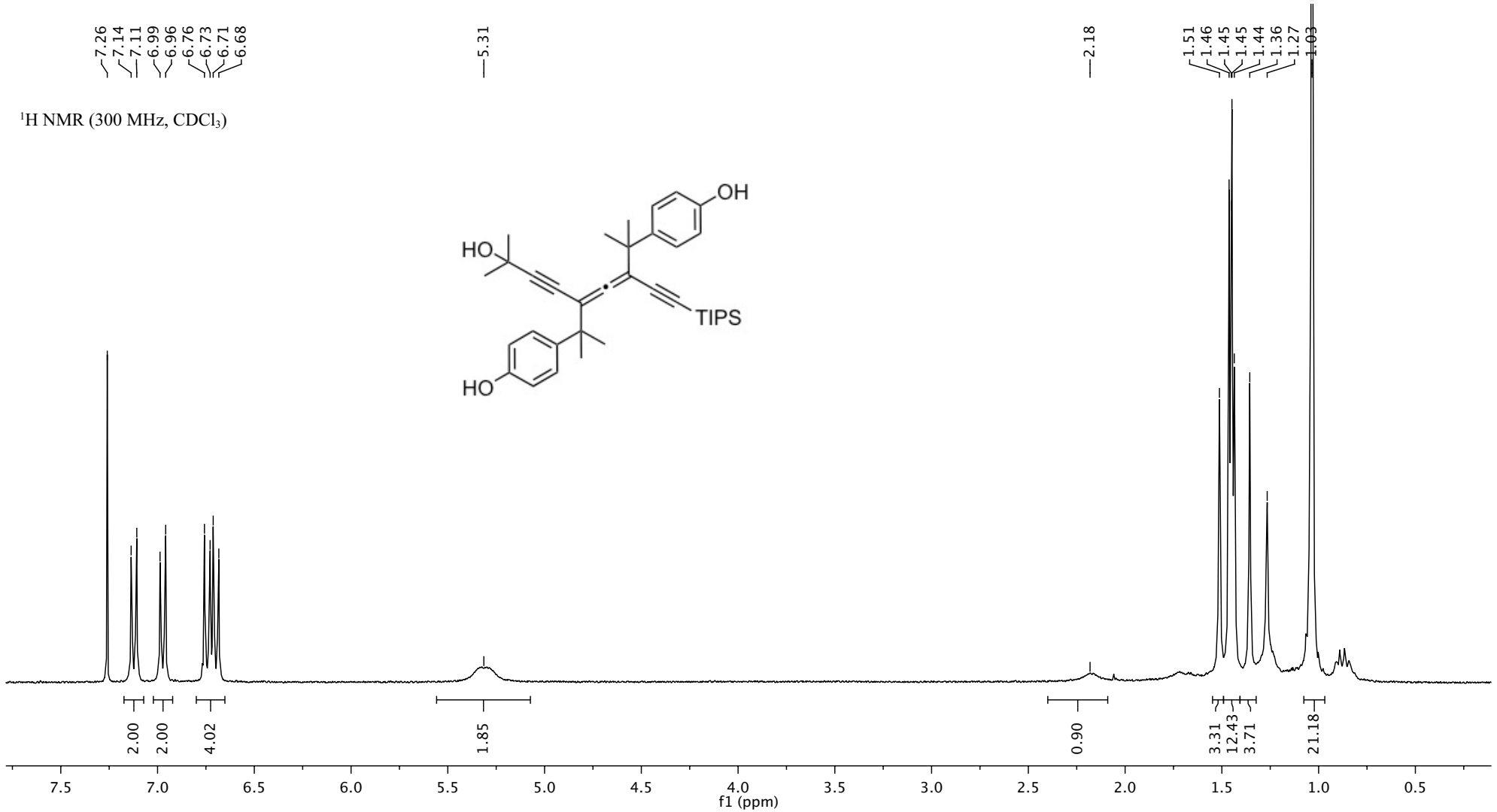

Figure S28. ^{1}H NMR (300 MHz, CDCl$_3$, 25 °C) spectrum of compound (±)-**7**.

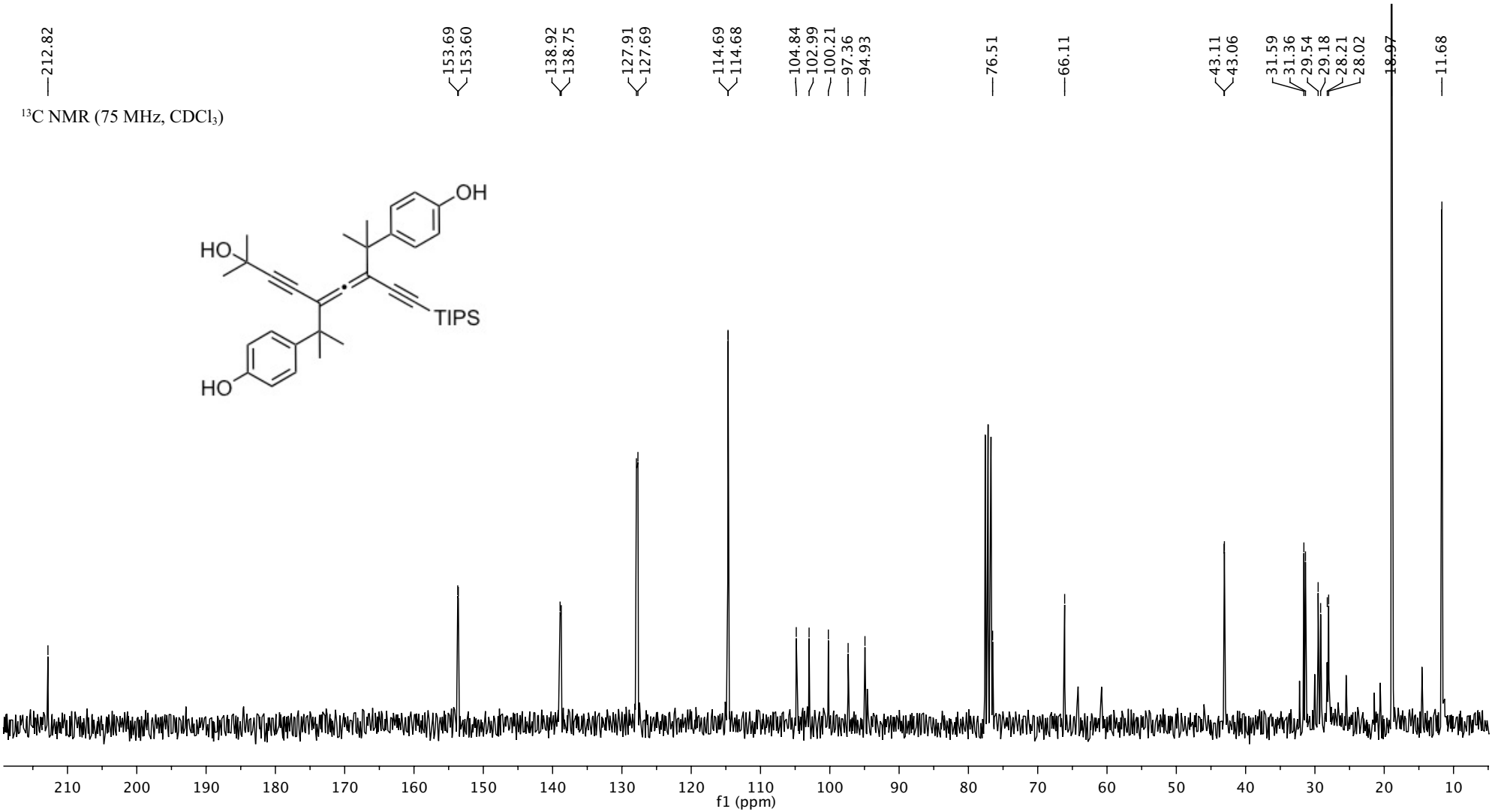

Figure S29. ^{13}C NMR (75 MHz, $CDCl_3$, 25 °C) spectrum of compound (±)-**7**.

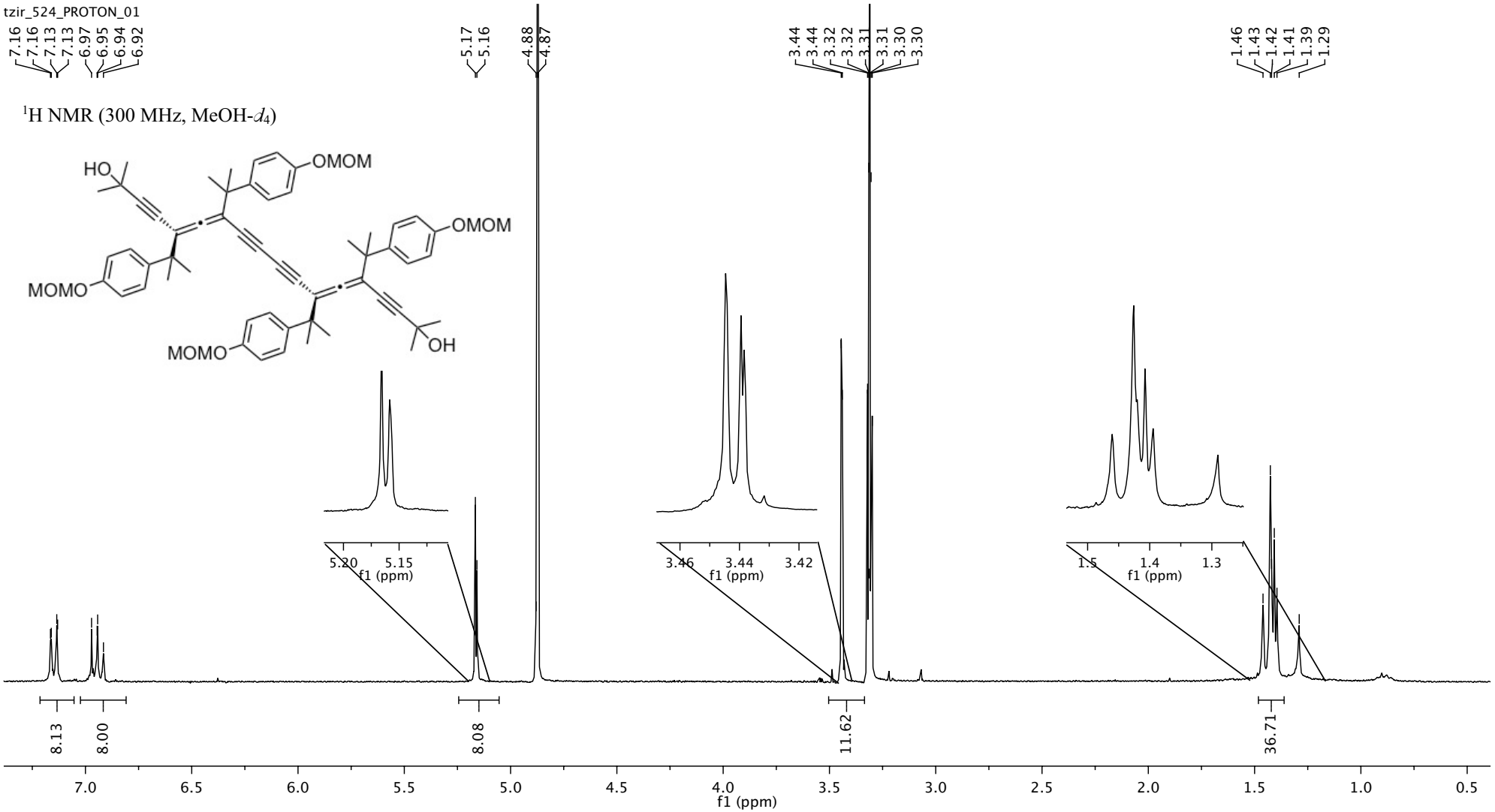

Figure S30. ^{1}H NMR (300 MHz, MeOH-d_4, 25 °C) spectrum of compound (*P,P*)-(+)-**9**.

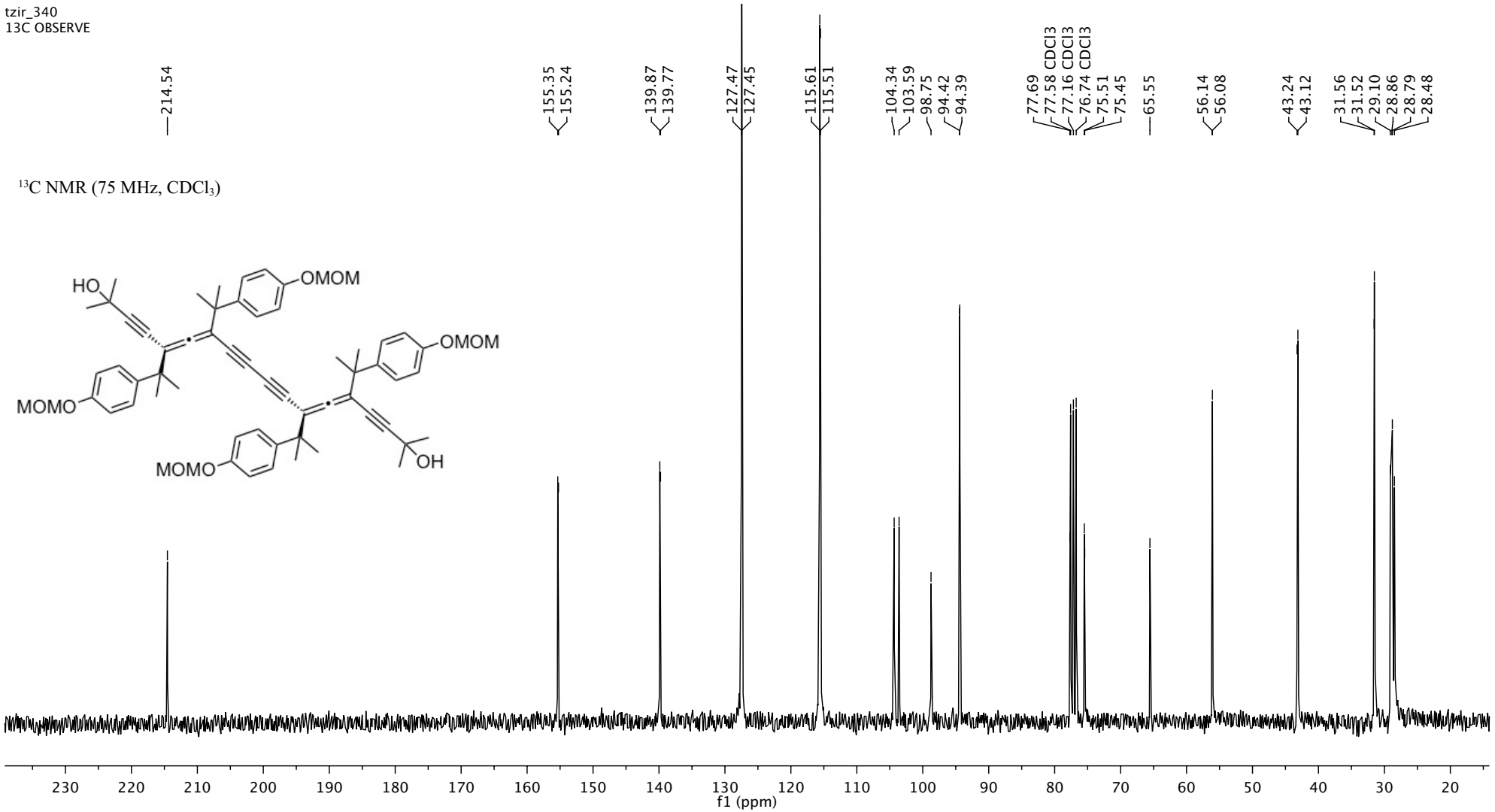

Figure S31. ^{13}C NMR (75 MHz, $CDCl_3$, 25 °C) spectrum of compound (*P,P*)-(+)-**9**.

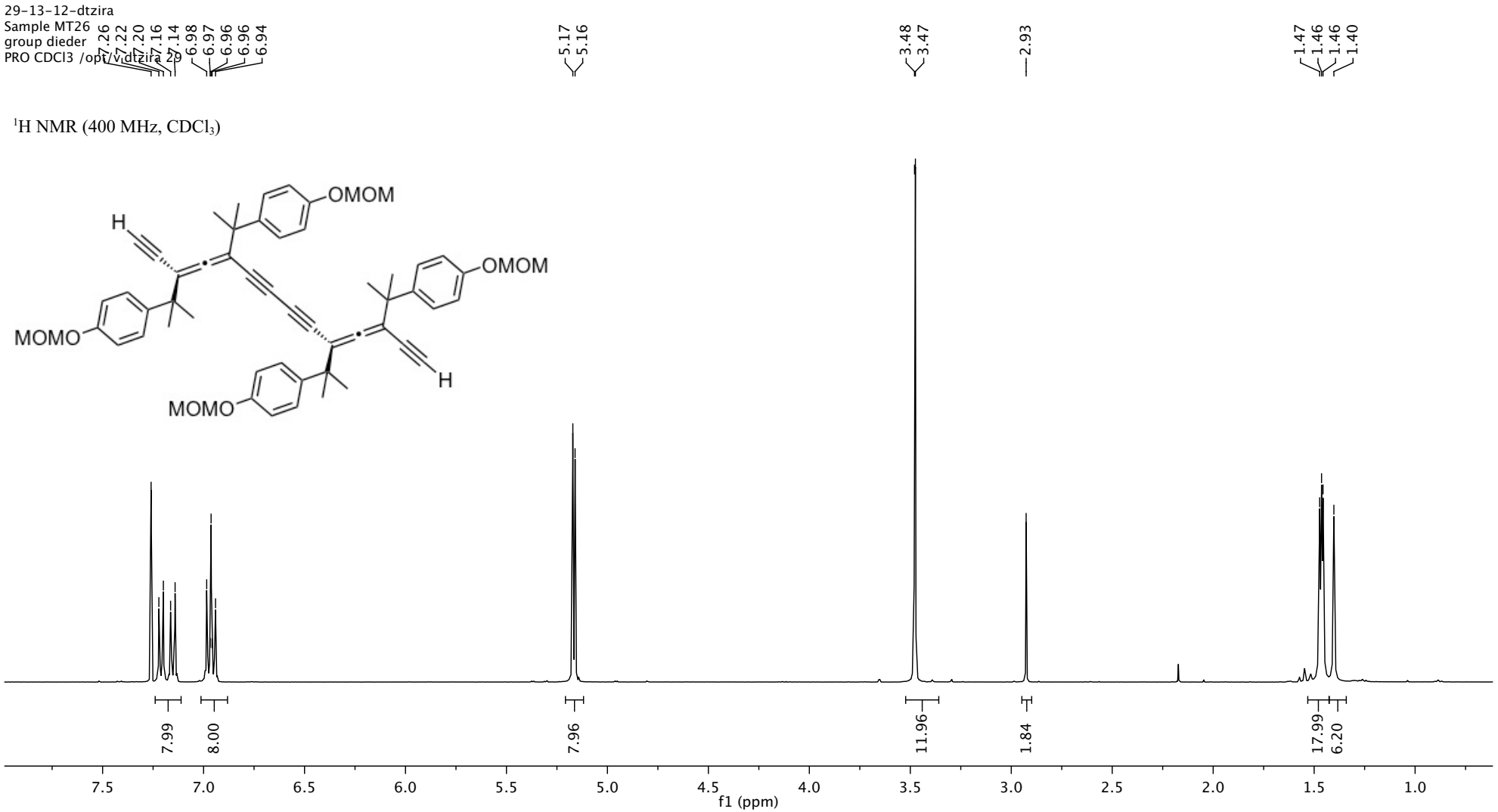

Figure S32. ^{1}H NMR (400 MHz, $CDCl_3$, 25 °C) spectrum of compound (*P,P*)-(+)-**10**.

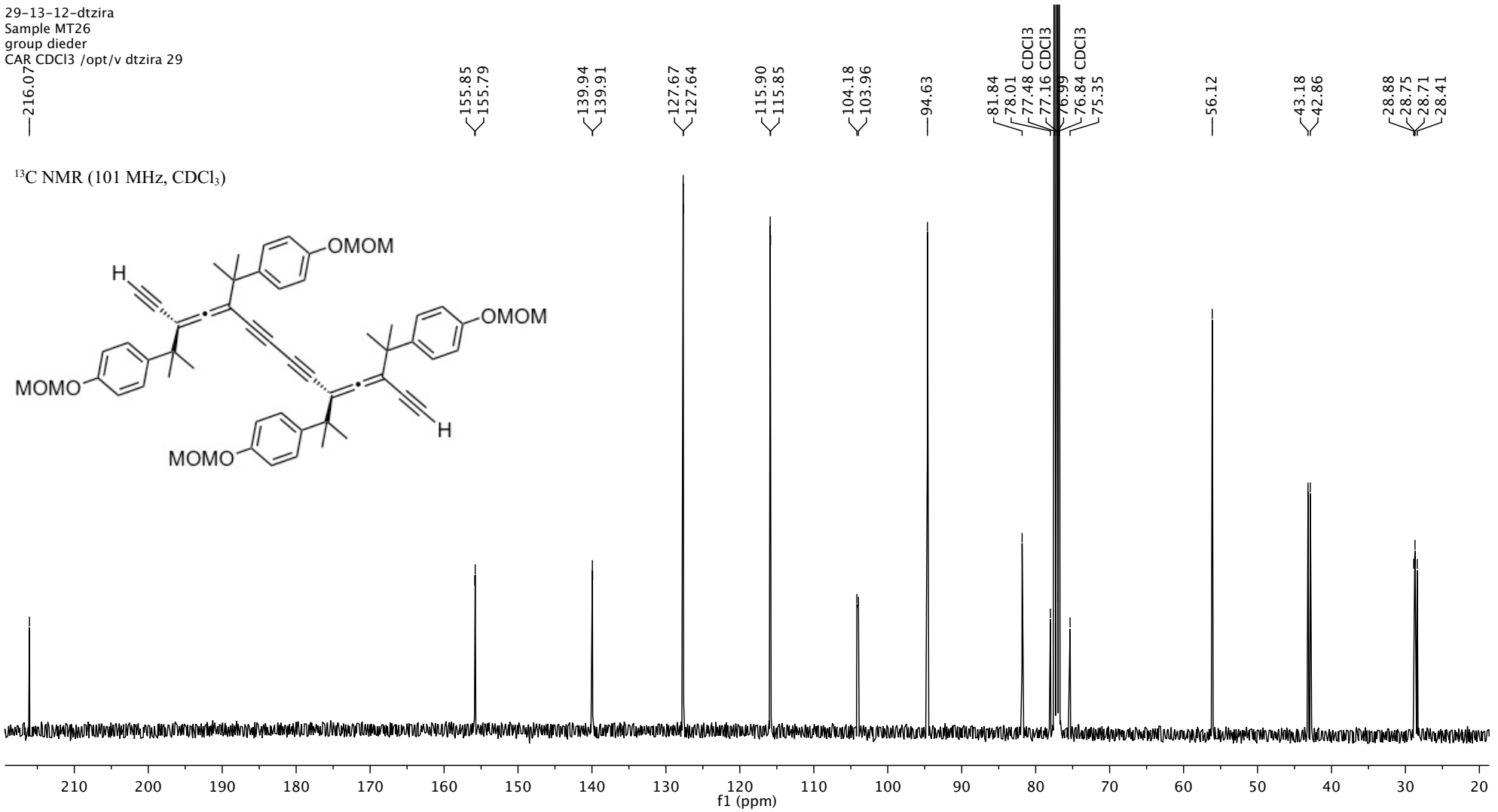

Figure S33. ^{13}C NMR (101 MHz, $CDCl_3$, 25 °C) spectrum of compound (*P,P*)-(+)-**10**.

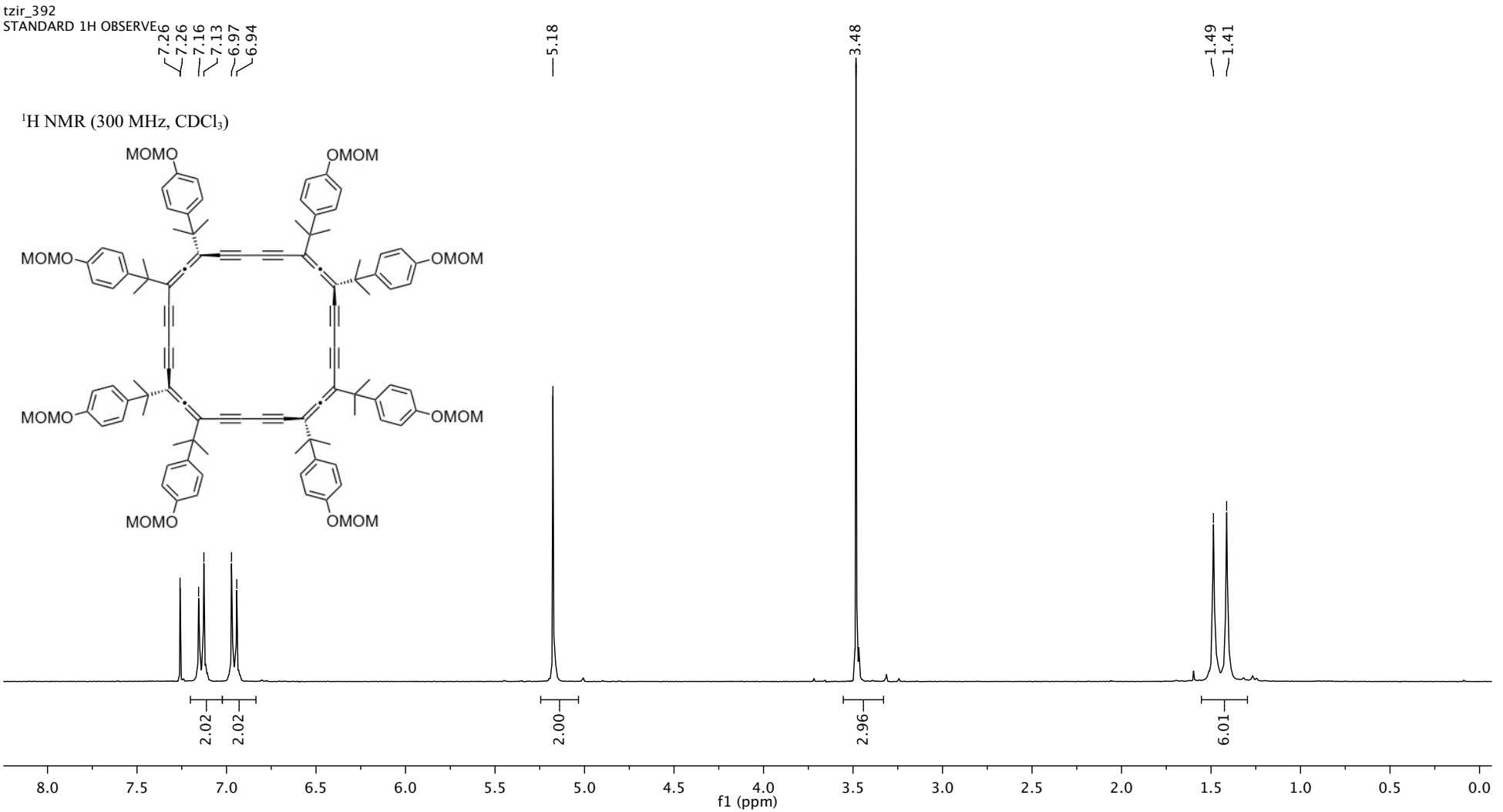

Figure S34. ^{1}H NMR (300 MHz, CDCl$_3$, 25 °C) spectrum of compound (*P,P*)-(+)-**11**.

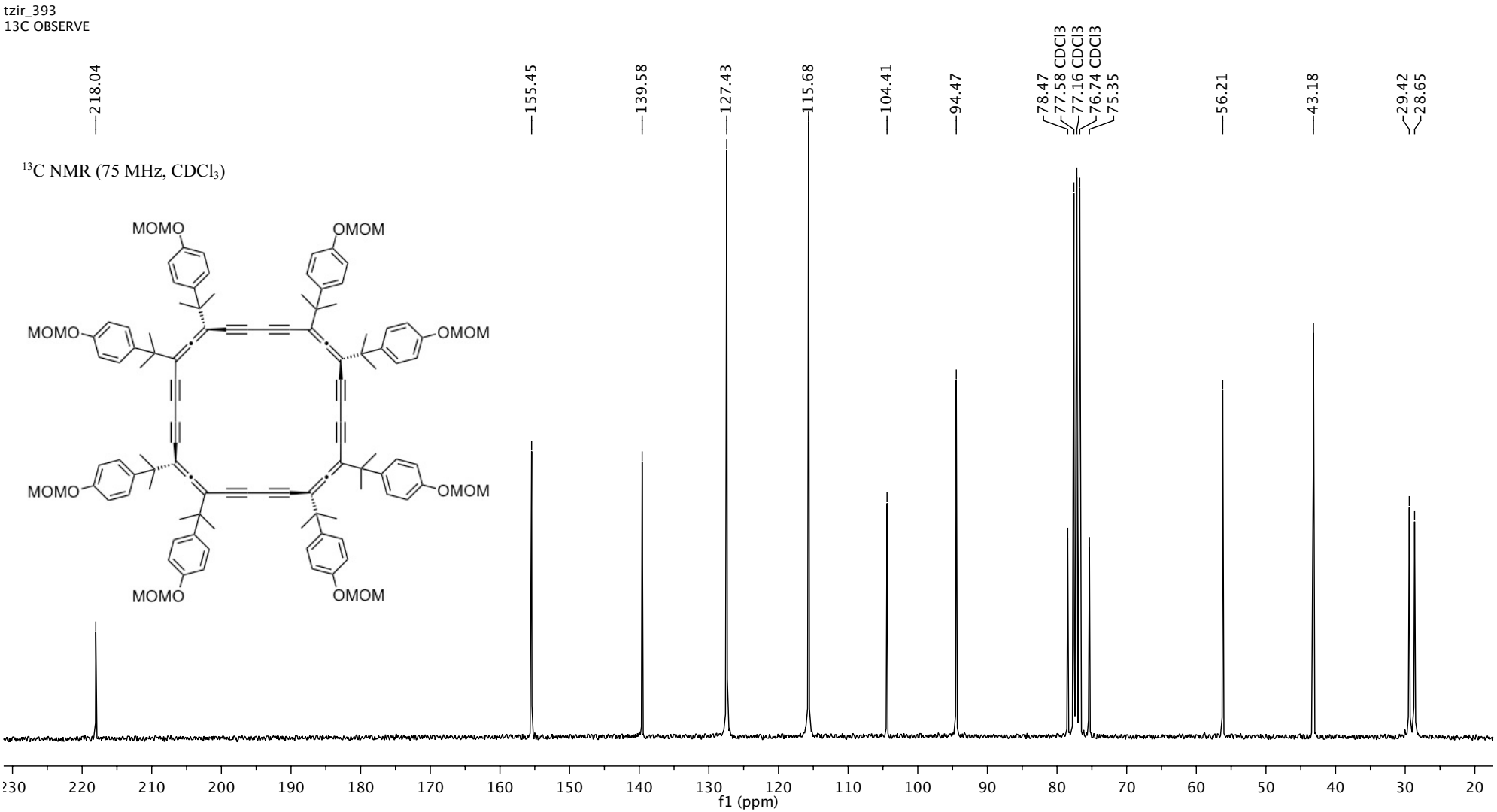

Figure S35. ^{13}C NMR (75 MHz, $CDCl_3$, 25 °C) spectrum of compound (*P,P*)-(+)-**11**.

10. References

1 M. K. J. ter Wiel, S. Odermatt, P. Schanen, P. Seiler and F. Diederich, *Eur. J. Org. Chem.*, 2007, 3449–3462.

2 J. L. Alonso-Gómez, P. Schanen, P. Rivera-Fuentes, P. Seiler and F. Diederich, *Chem.–Eur. J.*, 2008, **14**, 10564–10568.

3 G. M. Sheldrick, *Acta Cryst. A*, 2008, **A64**, 112–122.

4 P. Rivera-Fuentes, J. L. Alonso-Gómez, A. G. Petrovic, P. Seiler, F. Santoro, N. Harada, N. Berova, H. S. Rzepa and F. Diederich, *Chem.–Eur. J.*, 2010, **16**, 9796–9807.

5 (a) C. F. Macrae, P. R. Edgington, P. McCabe, E. Pidcock, G. P. Shields, R. Taylor, M. Towler and J. van de Streek, *J. Appl. Crystallogr.*, 2006, **39**, 453–457; (b) C. F. Macrae, I. J. Bruno, J. A. Chisholm, P. R. Edgington, P. McCabe, E. Pidcock, L. Rodriguez-Monge, R. Taylor, J. van de Streek and P. A. Wood, *J. Appl. Crystallogr.*, 2008, **41**, 466–470.

6 J. L. Alonso-Gómez, P. Rivera-Fuentes, N. Harada, N. Berova and F. Diederich, *Angew. Chem. Int. Ed.*, 2009, **48**, 5545–5548.

7 P. Rivera-Fuentes, J. L. Alonso-Gómez, A. G. Petrovic, F. Santoro, N. Harada, N. Berova and F. Diederich, *Angew. Chem. Int. Ed.*, 2010, **49**, 2247–2250.

8 Macromodel, Version 9.7, Schrödinger, LLC, New York, NJ, **2009**.

9 Rivera-Fuentes, B. Nieto-Ortega, W. B. Schweizer, J. T. L. Navarrete, J. Casado and F. Diederich, *Chem.–Eur. J.*, 2011, **17**, 3876–3885.